THE STREM CHEMIKER

Dedicated to Dr. Irving Wender on the occasion of his 90th birthday
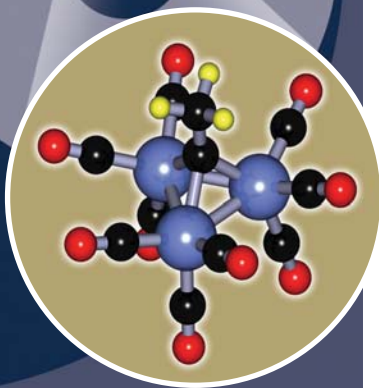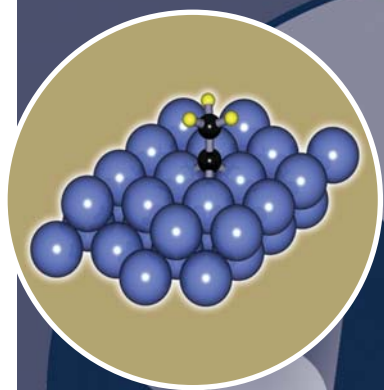
catalytic conversion of syngas

fuels and chemicals

organometallic chemistry

chemistry of carbon monoxide reactions

hydrogen economy

Includes technical articles by the speakers participating in the Wender Symposium held at the University of Pittsburgh, June 15, 2005

A Publication of Strem Chemicals, Inc.

Table of Contents

The Strem Chemiker
Vol. XXII No.1
November, 2005

www.strem.com

Dr. Irving Wender
Distinguished University
Research Professor

University of Pittsburgh

Department of Chemical and
Petroleum Engineering

When Mike Strem, the founder of Strem Chemicals Inc., was doing his graduate chemistry research at the University of Pittsburgh, his professor Dr. E. M. Arnett, suggested that they use cobalt carbonyl to trimerize acetylenes. Dr. Arnett mentioned that Irving Wender was an expert in the synthesis and chemistry of metal carbonyls and fortunately worked close-by at the U.S. Bureau of Mines in Bruceton, Pennsylvania.

At Dr. Arnett's urging, Mike spent a summer in Irving's lab learning to synthesize and use cobalt carbonyl. Interestingly, Mike was living with his parents at the time and Irving and his family lived just around the corner. They car-pooled for the summer, after which they continued their friendship and Irving mentored Mike on the possibility of founding a chemical company after graduate school. It turned into a reality, but not in Pittsburgh. The company started in Danvers, Massachusetts and later moved a few miles away to Newburyport where it stands today.

In June of 2005 Irving turned 90 years old. In celebration of this milestone, Mike sponsored a symposium in Irving's honor at the University of Pittsburgh. The articles in this edition of The Strem Chemiker have been submitted by the four plenary lecturers of the Wender Career Recognition Symposium 2005.

Born in New York, NY, on June 19, 1915, Irving Wender completed his undergraduate studies in chemistry at the College of the City of New York in 1936. His graduate work was interrupted by his induction into the Army, and he was sent to the University of Chicago to work on the Manhattan Project.

In 1945, Irving earned the Master of Science degree in chemistry from Columbia University. He was discharged from the Army in 1946 and joined the Chemistry Section of the U.S. Bureau of Mines in Pittsburgh, where he showed that coal could be treated as a complex organic substance in reactions.

As he pursued his Ph.D. at Pitt as well as later at the U.S. Bureau of Mines, Irving's discoveries in the areas of metal carbonyls and the "oxo" reaction (the catalyzed conversion of an alkene, carbon monoxide, and hydrogen to an aldehyde) won several awards. The Storch Award, for contributions to the science and utilization of coal, was awarded to him in 1964. Later in 1968, he won the Pittsburgh Award of the American Chemical Society, Pittsburgh Section for outstanding contributions to chemistry. The K.K. Kelley Award of the Department of Interior for contributions to coal chemistry and to catalysis followed in 1969.

In 1981, Dr. Wender was appointed research professor in Pitt's Department of Chemical and Petroleum Engineering. In 1982 he won the American Chemical Society's Award in Petroleum Chemistry for his work on metal carbonyls that led to a series of innovative findings fostering growth in the hydroformylation reaction. Today, plants using the hydroformylation reaction are in operation by oil, chemical and pharmaceutical companies. In 1988 he was the first recipient of the Homer H. Lowry Award, presented by the Secretary of Energy in Washington, D.C., "For his contributions in advancing fossil energy science and technology through highly innovative research on catalytic conversions of syngas to fuels and chemicals; creative determination of coal structure and conversion chemistry, and decisive guidance and inspirational leadership in shaping coal research programs in government, academia, and industry." In 1994, he was named Distinguished University Research Professor of Engineering at the University of Pittsburgh. In October 2002, he received the University of Pittsburgh's Department of Chemistry Alumni Award.

Dr. Wender has published over 200 papers. A life-long teacher, learner and researcher, his present studies are devoted to new ways of producing and storing hydrogen.

Keynote Lecturers and Speakers at the Wender Symposium and Contributing Authors of the Following Articles

Robert G. Bergman
Gerald E. K. Branch, Distinguished Professor of Chemistry, University of California at Berkeley

Donna G. Blackmond
Professor of Chemistry and of Chemical Engineering and Chemical Technology, Imperial College London, England

Götz Veser
Assistant Professor of Chemical and Petroleum Engineering, University of Pittsburgh

Tara Meyer
Associate Professor of Chemistry, University of Pittsburgh

2   Contact us for bulk or custom synthesis. Visit www.strem.com for new product announcements.

info@strem.com • technical@strem.com • quotation@strem.com • order@strem.com   3

C-H Activation and Sigmatropic Reactions Mediated by Inclusion in Supramolecular Assemblies

By D. Fiedler, D. Leung, K. N. Raymond and R. G. Bergman*

Department of Chemistry
University of California
Berkeley, CA 94720-1460, USA

*E-mail: rbergman@berkeley.edu

Following a period of exploration and mechanistic study, the activation of carbon-hydrogen bonds by metals[1] has become an important method of molecular synthesis in both commodities chemical research and applications for synthetic organic chemistry. At the same time, host-guest chemistry, the use of supramolecular assemblies as hosts for chemical reactivity, is emerging as an important way to study how binding molecules into space-restricted environments can mediate their chemical reactivity.[2-7] This article reports the preliminary results of a study designed to combine these two areas by utilizing the research interests and expertise of two groups at Berkeley, directed by R. G. Bergman and K. N. Raymond. This collaborative project has led to the finding that self-assembled molecular containers (so-called "nanovessels") are capable of encapsulating C-H activating organometallic molecules, thereby modifying their reactivity. Dramatic size and shape selectivities have been observed in this work. Subsequently, we have found that the nanovessel cavities are capable of functioning as catalytic sites for pericyclic reactions of organic molecules having appropriate substitution, shape and size.[8]

Background I: C-H Activation at Ir(III) Centers

Research on C-H activation reactions in the Bergman research group began in the early 1980s, when it was discovered that ultraviolet irradiation of complexes such as $Cp^*(PMe_3)IrH_2$ ($Cp^* = \eta^5\text{-}C_5(CH_3)_5$) resulted in reductive elimination of H_2, leading to transient, highly reactive Ir(I) intermediates capable of undergoing oxidative addition reactions with the C-H bonds of virtually any organic molecule R-H. This yields products of general formula $Cp^*(PMe_3)Ir(R)(H)$, in which the C-H bond in the organic molecule has been converted into new Ir-C and Ir-H bonds.[9] More recently, the group has discovered similar types of C-H activation reactions that occur in Ir(III) starting materials such as $Cp^*(PMe_3)Ir(R)(OTf)$ ($OTf = OSO_2CF_3 = $ triflate), leading to the type of replacement reactions shown in Scheme 1.[10-13] Extensive mechanistic work has revealed that these reactions take place by the mechanism illustrated in the Scheme, involving loss of triflate ion to give cationic intermediate **2**, followed by oxidative addition of a C-H bond in R-H to give Ir(V) intermediate **3**. Reductive elimination of methane and re-coordination of triflate ion results in product **5**.
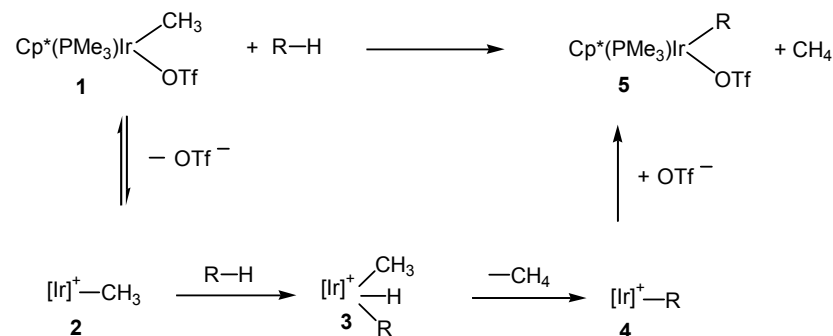
Scheme 1. Proposed mechanism for Ir(III) CH activation reactions ([Ir]= $\eta5\text{-}C_5Me_5$) $(PMe_3)Ir$).

Background II: M_4L_6 Tetrahedral Host-Assemblies

The Raymond group has recently synthesized and studied a series of chiral supramolecular coordination assemblies of M_4L_6 stoichiometry.[14-16] This system consists of four metal atoms (M = Ga^{3+}, Al^{3+}, In^{3+}, or Fe^{3+}) situated at the corners of a tetrahedron formed by six bridging (achiral) naphthalene based bis-bidentate catechol ligands (Figure 1). The negatively charged container molecule (overall charge -12) is soluble in water and other polar solvents, but contains a hydrophobic cavity of about 0.5 nm^3. It has been established that these vessels encapsulate a variety of monocationic species, among them NMe_4^+, NEt_4^+, PEt_4^+, Cp_2Co^+, and Cp_2Fe^+, to form host-guest complexes of the general formula $[G \subset M_4L_6]^{11-}$ ($\subset$ denotes guest encapsulation within the host).[17] The guest molecules' affinity for the cavity depends on their size, hydrophobicity, enthalpy of desolvation, and charge.
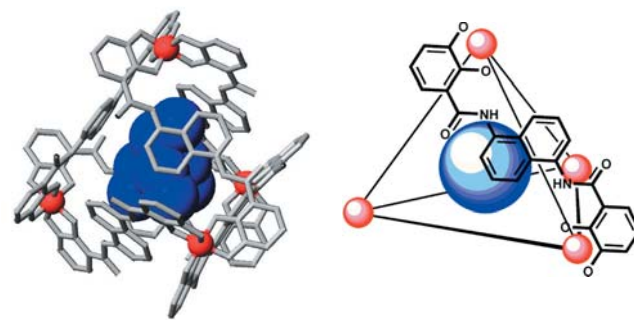

Figure 1. Left: Model of the crystal structure of $[NEt_4 \subset Fe_4L_6]^{11-}$. Right: Schematic of $[G \subset M_4L_6]^{11-}$. Six bis-bidentate catechol amide ligands span the edges of the tetrahedron (only one of the ligands is drawn for clarity).

Encapsulated Transition Metal Reactivity

Many organic transformations require the use of a transition metal catalyst, but reports on the mediation of these metal-catalyzed transformations by supramolecular encapsulation are relatively rare, and catalytic accelerations are often modest.[18-25]

4   Contact us for bulk or custom synthesis. Visit www.strem.com for new product announcements.

info@strem.com • technical@strem.com • quotation@strem.com • order@strem.com   5

The M_4L_6 assembly studied by Raymond et al. enables the supramolecular encapsulation of cationic transition metal complexes without the need to covalently tie them to a surrounding superstructure. This provides for the potential encapsulation of discrete reactive species within the same host assembly by simple addition of the host and guest in aqueous solution.

We first observed that half-sandwich ruthenium complexes were able to function as guests in the nanovessels.[26] Subsequent to that, we decided to explore the possibility that the half-sandwich iridium complexes synthesized by Bergman et al.[10, 11] could function as guests capable of intra-vessel C-H activation reactions. As mentioned above, the iridium(III) compound [Cp*(PMe$_3$)Ir(Me)OTf] (1) has been shown to thermally activate the C-H bonds of organic molecules at room temperature.[12, 13] Since these materials are soluble in water, and both the starting material and C-H activation transition state are monocationic, we hoped that encapsulation within the supramolecular host would allow for reaction and strong modification of organic reactant C-H activation selectivities.

The encapsulation of monocationic analogs of the iridium triflate species and its resulting reactivity were examined.[27] By substituting a dative ligand for the covalently bound triflate at the metal center, stable cationic 18 e$^-$ compounds of type [Cp*(PMe$_3$)Ir(Me)(L)][OTf] (L = donor ligand) can be prepared. The olefin adduct [Cp*(PMe$_3$)Ir(Me)(C$_2$H$_4$)][OTf] (6) was prepared by addition of ethylene to a solution of 1 in CH$_2$Cl$_2$ and is stable in aqueous solution, since the ethylene ligand is more strongly coordinated than water to the iridium center. However, one consequence of this stability is that 6 exhibits decreased reactivity compared to that of the neutral triflate species. Upon addition of aldehyde substrates to 6 in aqueous solution, no reactivity was observed until the solution was heated to 75°C.[12] However, at this temperature, a C-H activation/decarbonylation process occurred, analogous to that observed earlier with the corresponding triflate in dichloromethane solution. In the proposed mechanism of this reaction (Scheme 2), 6 first undergoes dissociation of ethylene. This generates the reactive 16 e$^-$ intermediate 7 (as in Scheme 1) that can activate the aldehydic C-H bond to release methane and form iridium acyl complex 8. Migratory deinsertion of CO from the acyl group gives the iridium alkyl carbonyl complex 9 as the final reaction product.[10, 28]
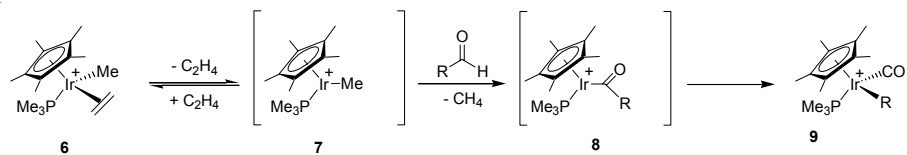
Scheme 2. Proposed mechanism of C-H bond activation of aldehydes by the iridium ethylene complex 12.

Combination of Na$_{12}$[Ga$_4$L$_6$] with 6 in aqueous solution resulted in immediate and quantitative encapsulation to form Na$_{11}$[6⊂Ga$_4$L$_6$]. This is revealed by the strong upfield shift of the NMR resonances of the encapsulated guest. In addition, since the iridium center is chiral, encapsulation by the chiral host assembly leads to the formation of two diastereomeric host-guest systems, which causes doubling of the ^{1}H NMR resonances

of encapsulated 6 (Figure 2). Molecular mechanics calculations on this system predicted an optimized structure in which 6 fits comfortably within the host cavity (Figure 2).[29] The reactive metal center is completely enclosed within the walls of the host, providing a tight, well-defined nanospace around the iridium species.
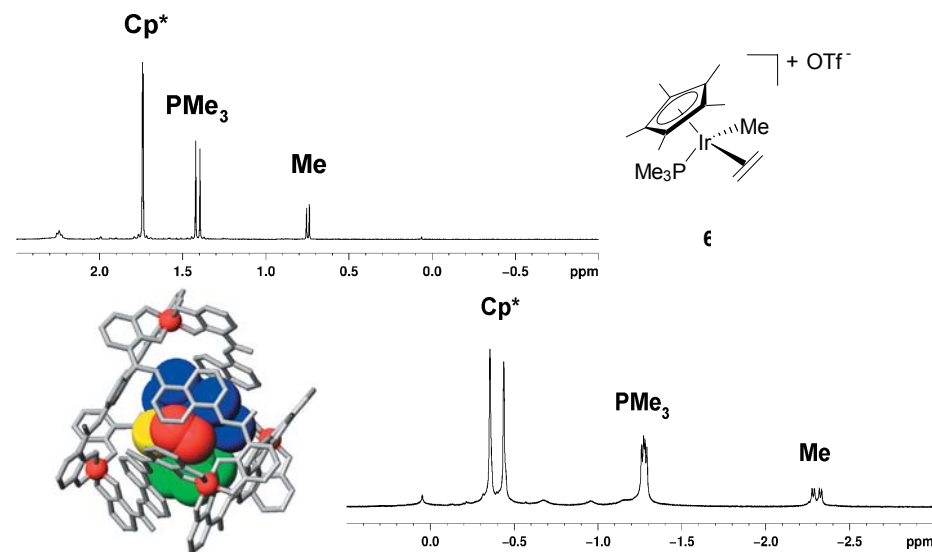

Figure 2. Top: ^{1}H NMR spectrum of unbound 6 D$_2$O. Bottom left: CAChe model of Na$_{11}$[6 ⊂ Ga$_4$L$_6$]. Bottom: ^{1}H NMR spectrum of Na$_{11}$[6 ⊂ Ga$_4$L$_6$] on the same axis. Two diastereomers are clearly distinguished.

Since the ethylene complex 6 displays C-H bond activation reactivity at 75° C, an analogous reaction of the corresponding host-guest assembly was explored. When acetaldehyde was added to an aqueous solution of Na$_{11}$[6 ⊂ Ga$_4$L$_6$] at this temperature, a new encapsulated product was obtained in moderate yield after several days. This new product was identified as the host-guest assembly [Cp*(PMe$_3$)Ir(Me)(CO) ⊂ Ga$_4$L$_6$]$^{11-}$, the product of the C-H bond activation of acetaldehyde (see top of Table 1). The product iridium carbonyl compound is also chiral, and was formed with a 60:40 diastereomeric ratio, even though there is lower diastereoselectivity observed in the original binding of 6.

The selectivity of the activation of aldehydes by the encapsulated iridium species was explored by examining a wide variety of substrates. The selectivity cutoffs exhibited by this system are remarkable (Table 1). The host-guest assembly Na$_{11}$[6 ⊂ Ga$_4$L$_6$] reacts with linear substrates ranging from acetaldehyde to n-butyraldehyde to form the corresponding encapsulated iridium carbonyl products. However, when the size of the aldehyde reaches valeraldehyde, no reaction is observed, presumably because the substrate is beyond the size regime allowed by the host cavity for reactivity. In

addition to the size constraints enforced by encapsulation, significant shape selectivity also was observed. The encapsulated iridium complex reacts with isovaleraldehyde but not with 2-methylbutanal: simply moving the branching methyl group from one carbon to an adjacent one dramatically changes the ability of the substrate to react with the host-guest assembly. This substrate selectivity can be observed *in situ* in a competition experiment with half of an equivalent of both acetaldehyde and benzaldehyde. When $Na_{11}[6 \subset Ga_4L_6]$ was added, upon heating, only the acetaldehyde substrate was activated, leaving benzaldehyde and half an equivalent of unreacted $Na_{11}[6 \subset Ga_4L_6]$ in solution. As the size of the linear aldehyde substrates is increased homologously from acetaldehyde to propionaldehyde to butyraldehyde, the diastereoselectivity of the activation reaction increases from 60:40 to 65:35 to 70:30. Thus increasing the size of the organic substrate interacting with the iridium center produces a correspondingly stronger chiral recognition by the host cavity.


Substrate	dr	Substrate	dr	Substrate	dr
	45 : 55		45 : 55		45 : 55
	40 : 60		42 : 58		n. r.
	30 : 70		n. r.		n. r.
	n. r.		n. r.		n. r.

Table 1. Observed reactions and diastereoselectivities in the C-H bond activation of aldehydes by the $Na_{11}[6 \subset Ga_4L_6]$ host guest assembly.

In considering the mechanism of the C-H activation of aldehydes with the encapsulated iridium complex, it is important to examine the possibility that the reaction takes place by reversible dissociation of **6** into aqueous solution, followed by reaction with aldehyde and then re-encapsulation of the product iridium carbonyl complex. The abrupt discontinuity in the dependence of reactivity on aldehyde size and shape discussed above provides evidence against this alternative mechanism. Experiments conducted in the absence of $[Ga_4L_6]^{12-}$ host demonstrated that unencapsulated **6** reacts with all of the aldehydes shown in Table 1 at similar rates. Therefore, in the C-H bond activation experiments carried out with the host-guest complex $[6 \subset Ga_4L_6]^{11-}$, if the iridium guest were leaving the host interior, no unusual selectivity should be seen among aldehydes of various shapes and sizes. However, just the opposite is observed—i.e., aldehydes that are too large or the wrong shape to enter and bind to the cationic metal center in the

substrate and product	k_{free} [s^{-1}]	$k_{encaps.}$ [s^{-1}]	acceleration
10a	3.49 x 10^{-5}	16.3 x 10^{-5}	5
10b	7.61 x 10^{-5}	198 x 10^{-5}	26
10c	3.17 x 10^{-5}	446 x 10^{-5}	141
10d	1.50 x 10^{-5}	109 x 10^{-5}	73
10e	0.37 x 10^{-5}	316 x 10^{-5}	854

Table 2. Rate constants for free and encapsulated reactions and their acceleration factors.
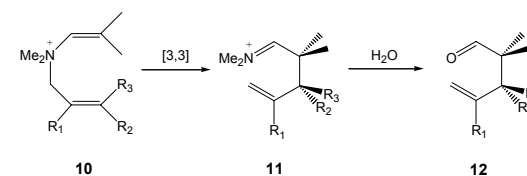
Scheme 3. General schematic for the 3-aza Cope rearrangement of enammonium cations (**10**) to iminium cations (**11**), followed by hydrolysis to yield γ,δ-unsaturated aldehydes (**12**).

iridium-containing cavity are completely protected from undergoing decarbonylation. We therefore conclude that the C-H bond activation reaction takes place within the host assembly.

Catalysis by Self-Assembled Hosts

Rather than encapsulating an organometallic catalyst into a container molecule for reaction with substrate, can the supramolecular host structure act alone as a catalyst? This is a relatively unexplored area for true container molecules; modest catalytic accelerations and product distribution improvements have been observed in a few cases.[30, 31]

The demonstration of catalyis of a unimolecular reaction within the tetrahedral metal-ligand assembly is an attractive goal. To that end, the cationic 3-aza Cope reaction seemed ideal. The reaction occurs thermally in *N*-allyl enamine systems, with varying degrees of facility depending on structural features, the cationic variant being more exothermic than the neutral version. The substrates are ammonium cations (**10** in Scheme 3), very similar to $NMe_2Pr_2^+$, which is known to be a strongly binding guest.[17]

The product of the rearrangement is an iminium cation (**11**), disposed to hydrolyze rapidly to the γ,δ-unsaturated aldehyde **12**. Since neutral molecules are bound weakly, or not at all, by the host-assembly, the aldehyde should be displaced rapidly by more enammonium substrate, potentially allowing for turnover.

The dimethylallyl-(2-methylpropenyl)ammonium cation (**10a**, R_1, R_2, R_3 = H) was encapsulated into the M_4L_6 assembly in aqueous solution to yield quantitatively $K_5(NMe_4)_6[\mathbf{10a} \subset Ga_4L_6]$.[32] The rearrangement of both the free and encapsulated enammonium cation was monitored by ^1H NMR spectroscopy in D_2O at 50°C in buffered solution (pD = 8.02). The rearrangement displayed clean first order kinetics for the disappearance of starting material. The rates of rearrangement for the free and encapsulated reaction differ: the encapsulated reaction is accelerated by about a factor of 5 (k_{free} = 3.49 x 10^{-5} s^{-1}; $k_{encaps.}$ = 16.3 x 10^{-5} s^{-1}). To explore the causes of the rate increase within the capsule, additional substrates were investigated. The rate constants for rearrangement (free and encapsulated) are summarized in Table 2. It is evident from these values that additional substituents on the enammonium cation enhance the rearrangement rate of encapsulated substrates, with factors of acceleration up to nearly 10^3.

Aware that the product of rearrangement is released from the cavity and hydrolyzes in aqueous solution, we explored the possibility of carrying out the reaction under catalytic conditions. Kinetic experiments with different catalyst loadings confirmed truly catalytic behavior of the self-assembled host for the 3-aza Cope rearrangement of **10c** (Figure 3). Raising the catalyst loading from 13 mol%, to 27 mol%, to 40 mol% resulted in the expected rate accelerations; the observed rate constants at 25ºC are $k_{13\%}$ = 0.64 x 10^{-4} s^{-1}, $k_{27\%}$ = 1.17 x 10^{-4} s^{-1}, $k_{40\%}$ = 1.80 x 10^{-4} s^{-1}.
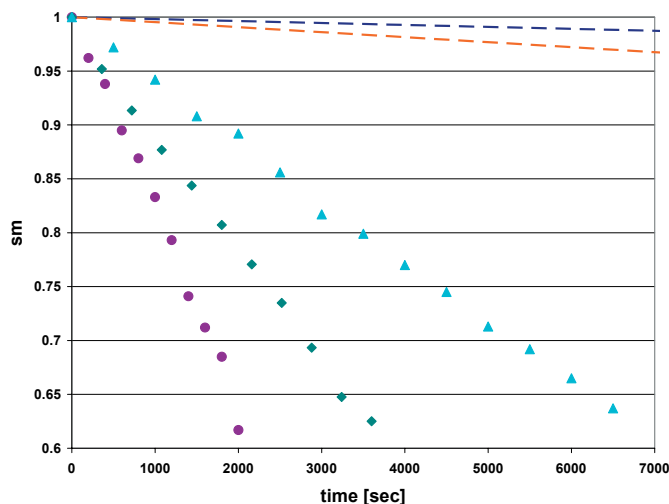

Figure 3. Initial rates at 25°C for the catalytic 3-aza Cope rearrangement of **10c**. ● = 40% catalyst loading; ◆ = 27% catalyst loading; ▲ = 13% catalyst loading; -- = 40% catalyst loading, inhibited with 8 eq. NEt_4^+; -- = uncatalyzed reaction.

Significantly, the addition of NEt_4^+, a very strongly binding guest that blocks the cavity interior, inhibited the reaction, we believe competitively. With this information, we propose the catalytic cycle depicted in Figure 4. First, the metal-ligand assembly binds the enammonium substrate into its cavity. This encapsulation orients the substrate in a reactive conformation, prone to rearrangement. The rearranged product is ejected from the cavity and hydrolyzes, allowing the next catalytic cycle to begin.
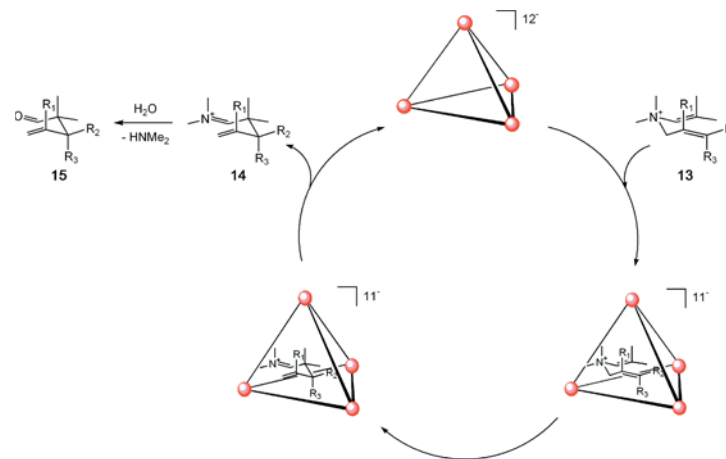

Figure 4. Proposed catalytic cycle of 3-aza Cope rearrangement, catalyzed by the metal-ligand assembly.

Future Perspective

The utilization of self-assembled supramolecular architectures as nanoscale reaction vessels is still in its infancy. Even though a broad range of such structures have been reported, their properties as catalytic reaction chambers rarely have been exploited. The results in this field represent a way to harness the method employed by enzymes in nature for use in synthetic applications to attain new selectivities beyond current techniques. The findings reported here display the features desired from a chiral nanoflask. Operating in aqueous solution, these metal-ligand assemblies are not only able to selectively bind their substrates, but also have proven their ability to control organometallic reactivity and mediate organic reactions catalytically. Future challenges include exploring the enantioselective induction of the resolved chiral host to achieve asymmetric catalysis and to increase the scope of reactivity within these supramolecular structures.

10   Contact us for bulk or custom synthesis. Visit www.strem.com for new product announcements.

info@strem.com • technical@strem.com • quotation@strem.com • order@strem.com   11

References

[1] For a review, see Shilov, A. E.; Shulpin, G. B. *Chem. Rev.* **1997**, *97*, 2879.

[2] Cram, D. J. *Nature* **1992**, *356*, 29-36.

[3] Lehn, J.-M. *Supramolecular Chemistry: Concepts and Perspectives*; VCH: Weinheim, 1995.

[4] Rebek, J. *Acc. Chem. Res.* **1999**, *32*, 278.

[5] Sauvage, J. P. *Acc. Chem. Res.* **1998**, *31*, 611.

[6] Fujita, M.; Fujita, N.; Ogura, K.; Yamaguchi, K. *Nature* **1999**, *400*, 52.

[7] Kang, J. M.; Rebek, J. *Nature* **1997**, *385*, 50-52.

[8] A significant portion of this material appeared in a recent issue of *Acc. Chem. Res.*: Fiedler, D.; Leung, D. H.; Raymond, K. N.; Bergman, R. G. *Acc. Chem. Res.* **2005**, *38*, 351.

[9] Asplund, M. C.; Snee, P. T.; Yeston, J. S.; Wilkens, M. J.; Payne, C. K.; Yang, H.; Kotz, K. T.; Frei, H.; Bergman, R. G.; Harris, C. B. *J. Am. Chem. Soc.* **2002**, *124*, 10605-10612, and references cited there.

[10] Arndtsen, B. A.; Bergman, R. G.; Mobley, T. A.; Peterson, T. H. *Acc. Chem. Res.* **1995**, *28*, 154-162.

[11] Klei, S. R.; Golden, J. T.; Burger, P.; Bergman, R. G. *J. Mol. Catal. A: Chem.* **2002**, *189*, 79-94.

[12] Burger, P.; Bergman, R. G. *J. Am. Chem. Soc.* **1993**, *115*, 10462-10463.

[13] Tellers, D. M.; Yung, C. M.; Arndtsen, B. A.; Adamson, D. R.; Bergman, R. G. *J. Am. Chem. Soc.* **2002**, *124*, 1400-1410.

[14] Caulder, D. L.; Bruckner, C.; Powers, R. E.; Konig, S.; Parac, T. N.; Leary, J. A.; Raymond, K. N. *J. Am. Chem. Soc.* **2001**, *123*, 8923-8938.

[15] Caulder, D. L.; Raymond, K. N. *Acc. Chem. Res.* **1999**, *32*, 975-982.

[16] Yeh, R. M.; Davis, A. V.; Raymond, K. N. In *Comprehensive Coordination Chemistry II*; McCleverty, J. A., Meyer, T. J., Eds.; Elsevier Ltd.: Oxford, UK, 2004; pp 327-355.

[17] Parac, T. N.; Caulder, D. L.; Raymond, K. N. *J. Am. Chem. Soc.* **1998**, *120*, 8003-8004.

[18] Slagt, V. F.; Reek, J. N. H.; Kramer, P. C. J.; Leeuwen, P. W. N. M. v. *Angew. Chem. Int. Ed.* **2001**, *40*, 4271-4274.

[19] Slagt, V. F.; Leeuwen, P. W. N. M. v.; Reek, J. N. H. *Angew. Chem. Int. Ed.* **2003**, *42*, 5619-5623.

[20] Slagt, V. F.; Kramer, P. C. J.; Leeuwen, P. W. N. M. v.; Reek, J. N. H. *J. Am. Chem. Soc.* **2004**, *126*, 1526-1536.

[21] Merlau, M. L.; Mejia, M. d. P.; Nguyen, S. T.; Hupp, J. T. *Angew. Chem. Int. Ed.* **2001**, *40*, 4239-4242.

[22] Morris, G. A.; Nguyen, S. T.; Hupp, J. T. *J. Mol. Catal. A: Chem.* **2001**, *174*, 15-20.

[23] Lee, S. J.; Hu, A.; Lin, W. *J. Am. Chem. Soc.* **2002**, *124*, 12948-12949.

[24] Jiang, H.; Hu, A.; Lin, W. *Chem. Commun.* **2003**, 96-97.

[25] Gianneschi, N. C.; Bertin, P. A.; Nguyen, S. T.; Mirkin, C. A.; Zakharov, L. N.; Rheingold, A. L. *J. Am. Chem. Soc.* **2003**, *125*, 10508-10509.

[26] Fiedler, D.; Pagliero, D.; Brumaghim, J. L.; Bergman, R. G.; Raymond, K. N. *Inorg. Chem.* **2004**, *43*, 846-848.

[27] Leung, D. H.; Fiedler, D.; Bergman, R. G.; Raymond, K. N. *Angew. Chem. Int. Ed.* **2004**, *43*, 963-966.

[28] Alaimo, P. J.; Arndtsen, B. A.; Bergman, R. G. *Organometallics* **2000**, *19*, 2130-2143.

[29] CAChe 5.04 ed.; Fujitsu Limited, 2002.

[30] Kang, J. M.; Santamaria, J.; Hilmersson, G.; Rebek, J. *J. Am. Chem. Soc.* **1998**, *120*, 7389-7390.

[31] Ito, H.; Kusukawa, T.; Fujita, M. *Chem. Lett.* **2000**, *29*, 598-599.

[32] Fiedler, D.; Bergman, R. G.; Raymond, K. N., unpublished results.

Kinetic Investigations of the Role of Catalysis in the Origin of Biological Homochirality

Donna G. Blackmond
Department of Chemistry
Department of Chemical Engineering and Chemical Technology
**Imperial College**
London SW7 2AZ

Optical activity is a widespread property of molecules constituting living matter. Optically active substances have been isolated in oils derived from coal, which is produced from the progressive fossilization of plant materials.[1] The origin of biological homochirality is a question that has intrigued scientists ever since the importance of L-amino acids and D-sugars was first recognized. The problem has two parts: 1) how might asymmetry initially develop? and 2) how might a minute initial imbalance be amplified to the high levels of enantiopurity inherent in modern biological systems?

The first part of the problem has been discussed recently in a lucid review by Mislow[2], who points out that it has been known for more than a century, if not generally recognized, that absolute asymmetric synthesis is achievable *without* chiral intervention, merely as a result of statistical fluctuations. Potential solutions to the second part of the problem were delineated half a century ago by Frank[3] and by Calvin[4]. It was suggested that asymmetric autocatalytic processes might have played a role in the development of high optical activity in biomolecules. Frank's work showed that if one hand of a primitive asymmetric catalyst could act to replicate itself and, at the same time, act to suppress replication of its opposite enantiomer, this would provide a "simple and sufficient life model" to explain how homochirality could have developed in the prebiotic world. The final sentence of this purely theoretical work presented, in the words of Hans Wynberg[5], "a challenge to all red-blooded chemists": Frank commented that a laboratory demonstration of his model "may not be impossible."

Some 40 years later, Kenso Soai answered Frank's challenge with the discovery that the alcohol product of the diisopropylzinc alkylation of pyrimidyl aldehydes catalyzes its own production at a much greater rate than it does the production of its enantiomer (Scheme 1)[6, 7, 8]. The ramifications of Soai's work have the potential to speak to the heart of some of our most intriguing questions about the chemical origin of life on Earth.

Scheme 1.
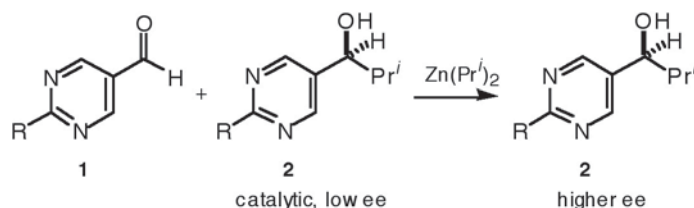
While the Soai reaction serves as a mechanistic model[9] for the evolution of homochirality from nearly racemic sources, the specific dialkylzinc chemistry involved in these reactions is unlikely to have been of importance in an aqueous prebiotic environment. Therefore, speculation has continued concerning the types of transformations that might have been directly responsible for the development of high optical activity in biological systems. The area of amino acid catalysis such as the reactions shown in Scheme 2[10, 11], may hold significant clues to the evolution of prebiotic chemistry. That prebiotic building blocks such as sugars can be formed with asymmetry from such reactions has recently led to speculation about the evolution of biological homochirality via such routes.[12]

Scheme 2.
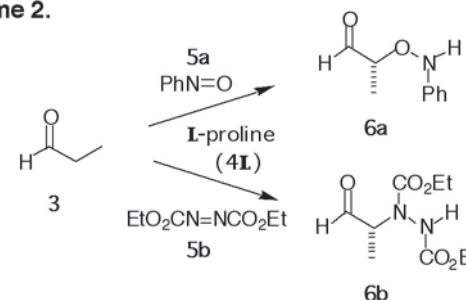
Such autocatalytic and autoinductive processes exhibit complex temporal reaction progress profiles, featuring time-dependent product selectivities and catalyst concentrations. One key to understanding autocatalytic and autoinductive effects lies in finding accurate methods for analyzing the progress of these reactions. Mechanistic studies by our group of the reactions in Schemes 1 and 2 have focused on detailed reaction progress kinetic analysis[13]. Selected results from our work on each reaction system are described after a short introduction to the kinetic methodology employed.

Kinetic Studies Using Reaction Calorimetry

Reaction calorimetry is a powerful in-situ tool for obtaining temporal rate profiles. This technique relies on the accurate measurement of the heat evolved or consumed when chemical transformations occur. If a catalytic reaction proceeds in the absence of side reactions or other thermal effects, the measured heat flow is directly proportional to the reaction rate. Each time a substrate molecule is transformed into a product molecule, an energy characteristic of that transformation—the heat of reaction, ΔH_{rxn}—is manifested. The proportionality constant between the heat evolved and the reaction rate is simply this thermodynamic heat of reaction. The quantity of heat evolved up to at any given time during the reaction may be compared to the total heat evolved when all the molecules have been converted. This ratio gives the fractional heat evolution, which is identical to the fraction conversion of the limiting substrate.

A heat flow curve for a proline-mediated aldol reaction is illustrated in Figure 1a. Figure 1b highlights the key component that makes kinetic analysis by this method work, namely, validation that the heat we are measuring corresponds accurately to the reaction of the molecules in question. If two or more separate techniques are employed (here we compare reaction calorimetry with FTIR spectroscopy and GC analysis of

14   Contact us for bulk or custom synthesis. Visit www.strem.com for new product announcements.

info@strem.com • technical@strem.com • quotation@strem.com • order@strem.com   15

samples extracted from the reactor), and if these separate experiments provide identical profiles of fraction conversion vs. time, we are assured that the reaction calorimetric method is a valid and accurate measure of the rate of the reaction under study.
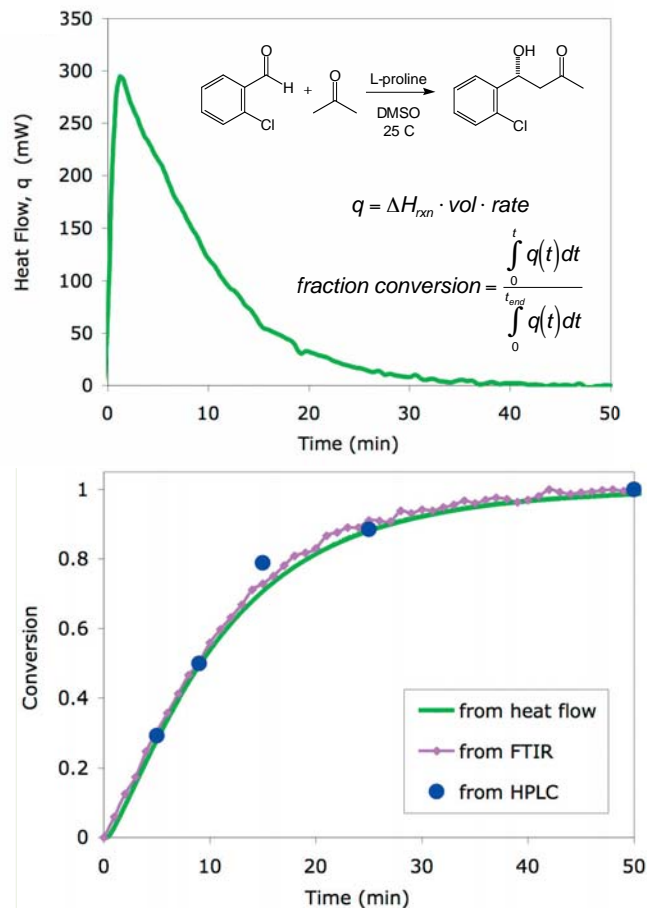

Figure 1. a) Reaction calorimetric monitoring of a proline-mediated aldol reaction; b) comparison of fraction conversion in this reaction measured from the reaction calorimetric heat flow to that measured by monitoring with FTIR spectroscopy and by sampling followed by HPLC analysis. The close agreement in conversion measured by different techniques validates the use of reaction calorimetry as a kinetic tool for monitoring this reaction.

Reaction calorimetry measures a property that is proportional to the instantaneous *difference* in substrate concentration over an infinitesimal time interval. This may be compared to more conventional *integral* measurements such as FTIR or NMR

spectroscopy that measure concentration directly. Difference methods offer an advantage over integral methods because instantaneous differences are easier to perceive than are cumulative changes in a temporal profile. These features may be particularly important in studying reactions such as those of Schemes 1 and 2, as is illustrated in the next sections.

Kinetic Studies of the Soai Reaction

Figure 2 shows the kinetic profile of the Soai reaction of Scheme 1 obtained from reaction calorimetric monitoring. The data are plotted in two different ways. Figure 2a shows the direct measurement of rate vs. fraction conversion. In this plot we can clearly see the autocatalytic behavior, with reaction rate rising as catalyst is produced, until an inflection point is reached at ca. 28% conversion. At higher conversions the rate declines as the rate of production of new catalyst is outweighed by the rate of consumption of the substrates.

In Figure 2b, the same data are plotted as fraction conversion vs. reaction time, as would be obtained in an FTIR or NMR spectroscopic experiment. Here we see that the inflection point is much more difficult to pick out by eye. In addition, we can see that when we look at a plot of conversion vs. time as in Figure 2b, we inadvertently place more emphasis on data obtained at high conversion than we do with a plot of rate vs. conversion as in Figure 2a.
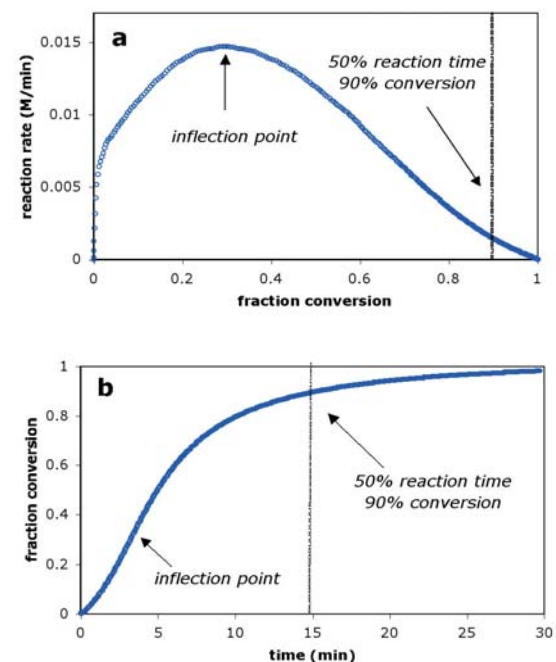

Figure 2. Reaction calorimetric kinetic profile of the Soai reaction of Scheme 1, with the same data plotted as: a) reaction rate vs. fraction conversion; and b) fraction conversion vs. time.

By removing time as an explicit variable, the y and x axes of the plot in Figure 2a represent the same quantities we find on the left and right sides of the equality sign in a reaction rate equation. Therefore we term a plot of this type a **"graphical rate equation."** Eq. 1 shows this for the simple model example of a reaction that exhibits first order kinetics in the concentration of substrate A.

$$rate = k \cdot [A] = k \cdot [A]_0 \cdot (1-f)$$

(1) $y - axis = rate; \quad x - axis = conversion, \ f$

a

b
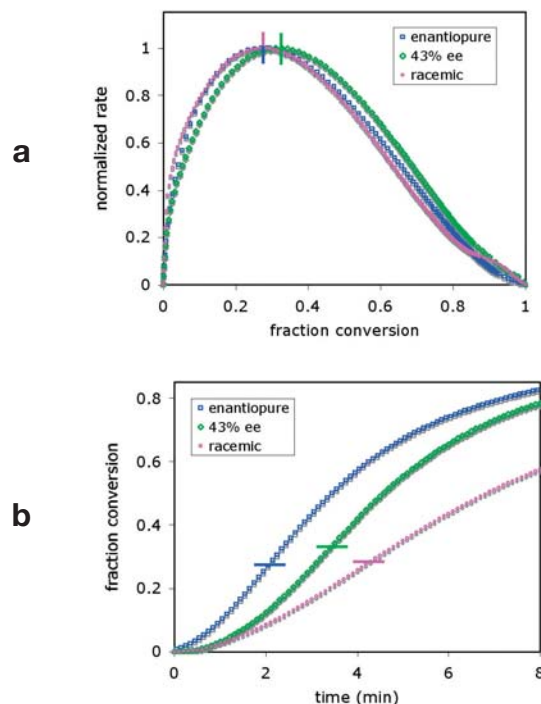
Figure 3. Reaction calorimetric kinetic profiles of the Soai reaction of Scheme 1 for autocatalyst **2** employed at ee = 100% (blue squares), 43% (green diamonds) and 0% (magenta circles). Data are plotted as normalized reaction rate vs. fraction conversion in the left figure and as fraction conversion vs. time in the right figure. Horizontal and vertical lines indicate the inflection point where reaction rate stops rising.

Such graphical representations of the kinetic data provide a wealth of mechanistic clues about more complex reactions such as the Soai reaction of Scheme 1. Figure 3a shows the interesting relationship we observed in our "graphical rate equations" comparing reactions carried out using enantiopure, scalemic, and racemic catalyst **2.**

Scheme 3.

$$K_{dimer} = \frac{[SR]^2}{[SS]^0[RR]} = 4$$

inactive heterochiral dimer reservoir

homochiral dimer catalysts
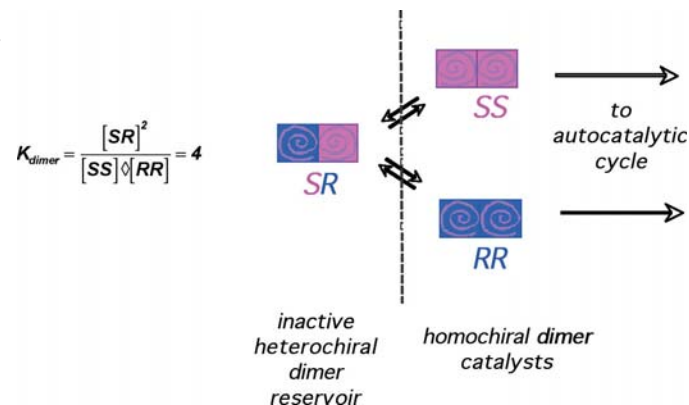
When the rate profiles are overlaid by normalizing the rate, we can see clearly that the inflection point occurs at *identical* conversion for enantiopure and racemic **2**, but is shifted to slightly higher conversion for 43% ee **2**. The same data are shown in Figure 3b with the inflection point marked by the horizontal bars. Extracting this important relationship between the data is clearly much more difficult working from the integral representation of the data.

This relationship was key to our proposal of a mechanistic model for the Soai reaction suggesting that the reaction is catalyzed by dimers of **2** that form in a statistical distribution of homochiral and heterochiral species, and that only the homochiral dimers are catalytically active as shown in Scheme 3. Modifying Kagan's ML_2 model[14] for nonlinear effects for the case of an autocatalytic reaction allowed us to predict the temporal increase in product (catalyst) enantiomeric excess over the course of the reaction. This is shown in Figure 4 for two reactions commencing with species **2** at 6% and 22% ee, respectively. The filled circles represent ee values determined from sampling the reaction vial and analyzing by HPLC. The magenta lines are *not*, however, simply "best fit" lines through these experimental data points; these lines derive from the kinetic model's *prediction* of product ee based solely on the *experimental reaction rate data*! The fact that the experimental rate data in this highly complex autocatalytic reaction can predict the observed asymmetric amplification with such breathtaking accuracy provides both strong support for the mechanistic model and a clear endorsement of the experimental kinetic methods employed.

This kinetic analysis reveals the striking conclusion that an overwhelming asymmetric amplification is possible in an *autocatalytic* system without invoking a stereochemical bias in dimer formation. This is in contrast to catalytic systems exhibiting nonlinear effects, where strong nonlinear effects occur require the heterochiral dimer to be significantly more stable than the homochiral dimers. This fact may be what gave the prebiotic soup of simple molecules a running chance at achieving homochirality in the absence of template molecules of complex stereochemical architecture.
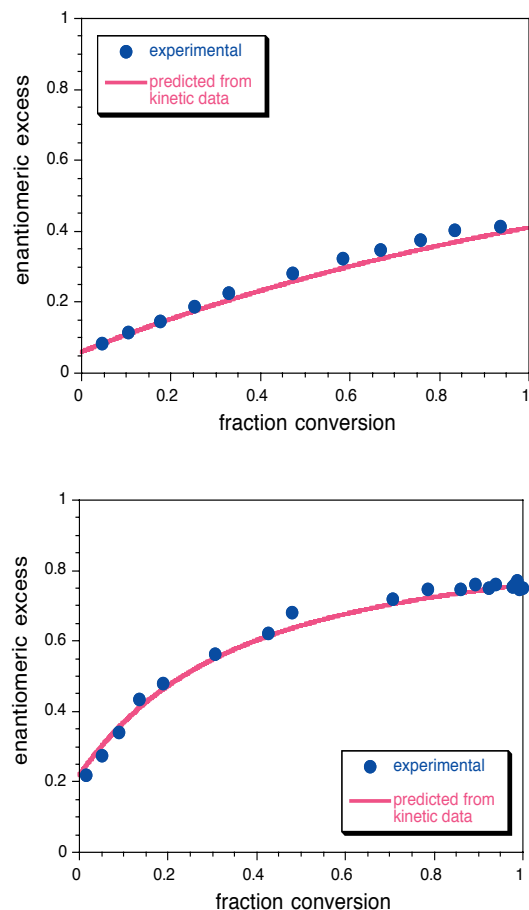
Figure 4. Experimental and predicted enantiomeric excess of **2** over the course of the Soai autocatalytic reaction of Scheme 1 carried out using enantioimpure **2** as catalyst (left: 6% ee **2**; right 22% ee **2**). The magenta lines give the temporal enantiomeric excess predicted from fitting experimental rate data to the kinetic model with dimer equilibrium constant K = 4 (statistical distribution) and inactive heterochiral dimer.

Proline Mediated Reactions

Asymmetric aminocatalysis has emerged as a successful vehicle for accomplishing a wide variety of highly enantioselective organic transformations[15]. Mechanistic analogies to enzymes[16], including the importance of hydrogen bonding[17], have recently been highlighted in a number of cases. The reactions shown in Scheme 2 are two recent additions to the rapidly expanding list of proline-based reactions introduced with the discovery of the Hajos-Parrish-Eder-Weichert-Sauer reaction[18] and elegantly revived by List et al.[19] with the intermolecular aldol reaction.

Our initial kinetic and mechanistic studies showed that the reactions of Scheme 2
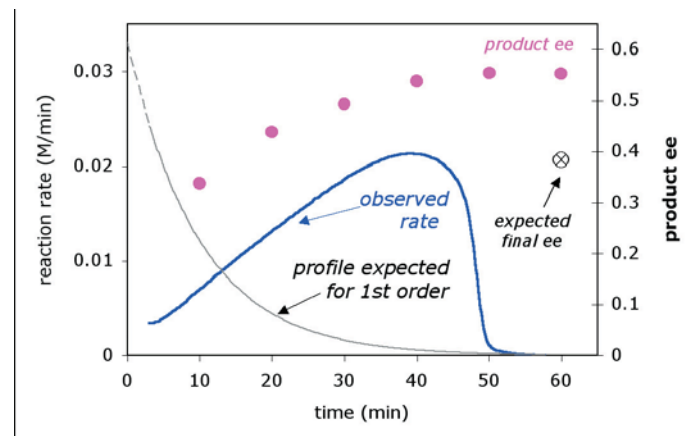
Figure 5. Reaction rate and ee as a function of time in the reaction in Scheme 2 (with **1a**) carried out using 40% ee L-proline. The rate was observed to rise (blue line), rather than fall (expected for first order kinetics, grey line), as substrate was consumed. The enantiomeric excess, which rose over the course of the reaction (pink circles) was higher than that predicted based on the proline ee (x in circle).
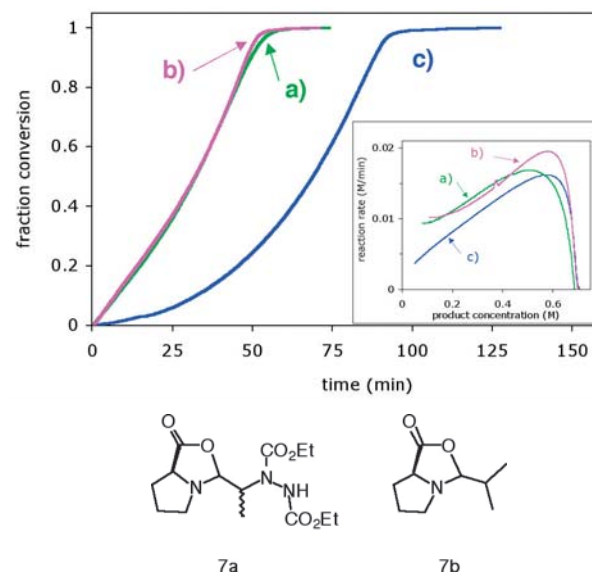
Figure 6. Fraction conversion vs. time for the amination reaction of Scheme 2b catalyst a) 10 mol% **7b**; b) 10 mol% **5c**; c) 20 mol% 4L; Inset: reaction rate vs. product concentration for the reactions shown in the main figure.

exhibit an accelerating rate that is proportional to product concentration[20]. In addition, the reaction exhibits asymmetric amplification when carried out using non enantiopure proline. These features are shown in Figure 5. We proposed that a hydrogen-bonded product-proline adduct acts to help solvate proline in low dielectric solvents, providing an effective increase in catalyst concentration in organic solvents where amino acids are themselves generally only sparingly soluble.

Figure 6 allows us to highlight another case in which a "graphical rate equation" provides us with enhanced mechanistic insight. The main part of the plot compares fraction conversion vs. time for proline and the soluble proline oxazolidinones **7a** and **7b** as catalysts. The slopes of the curves in a) and b) for the soluble catalyst look *almost* straight, a fact that would indicate overall zero-order kinetics. However, viewing the same data as rate vs. product concentration (Figure 6 inset) shows that these soluble catalysts also exhibit rate acceleration, and—most importantly—that rate acceleration is *proportional to product concentration* for both proline and these soluble derivatives.

Removing the explicit time scale from the data in Figure 6 provides a new perspective that offers tantalizing mechanistic clues, implying a role for the reaction product that goes beyond simple solvation. These results suggest that an interaction between the reaction product and the proline catalyst help make the system more efficient. Understanding this interaction may help us understand how small molecule amino acid catalysts evolved into highly efficient enzymes. Consider, for example, the chemically austere environment of a simple prebiotic catalyst. With meager resources available to undergo structural alterations that improve catalytic performance, where better for the catalyst to start than with the product molecule it just generated? A reaction product that itself may act to enable a higher efficiency catalytic cycle may reveal an important tool for evolutionary improvement in the development of primitive amino acid catalysts.

Afterword

The use of detailed kinetic analysis from an accurate differential method of measuring rate has been shown to provide significant insight into autocatalytic and autoinductive reactions that may ultimately contribute to our understanding of the origin and evolution of biological homochirality.

References
[1]   Zahn, C.; Langer, S.H.; Blaustein, B.D.; Wender, I. *Nature*, **1963**, *200*, 53.
[2]   Mislow., K. Collect. Czech. Chem. Commun., **2003**, *68*, 849-864.
[3]   Frank, F.C. *Biochim. Biophys. Acta,* **1953**, *11*, 32.
[4]   Calvin, M. Molecular Evolution," OUP, Oxford, 1969.
[5]   Wynberg, H., J. *Macromol. Sci.-Chem.*, **1989** *A26*, 1033.
[6]   Soai K.; Shibata T.; Morioka H.; Choji K. *Nature* **1995**, *378*, 767-768.
[7]   Shibata T.; Choji K.; Hayase T.; Aizu Y.; Soai K. *Chem. Commun.* **1996**, 1235-1236.
[8]   Shibata T.; Morioka H.; Hayase T.; Choji K.; Soai K. *J. Am. Chem. Soc.* **1996**, *118*, 471-472.
[9]   a) D. G. Blackmond, C. R. McMillan, S. Ramdeehul, A. Schorm, J. M. Brown. *J. Amer. Chem. Soc.* **2001**, *123*, 10103; b) D. G. Blackmond. *Adv. Synth. Catal*. **2002**, *344*, 156; c) F. G. Buono, D. G. Blackmond. *J. Amer. Chem. Soc.* **2003**, *125*, 8978; d) F.G. Buono, H. Iwamura, D.G. Blackmond. *Angew. Chemie. Int. Ed.*; **2004**, *43*, 2099; e) Blackmond, D.G. *PNAS*, **2004**, *101*, 5732*;* f) I.D. Gridnev, J.M. Serafimov, H. Quiney, J.M. Brown. *Org. Biomolec. Chem.* **2003**, *1*, 3811. g) I.D. Gridnev, J.M. Serafimov, J.M. Brown. *Angew. Chemie.* **2004**, *43*, 2884. h) I.D. Gridnev, J.M. Brown. *PNAS.* **2004**, *101*, 5727.
[10] a) Zhong, G. *Angew. Chemie. Int. Ed.*, **2003**, *42*, 4247; b) S. Brown, M. Brochu, C.J. Sinz, D.W.C. MacMillan. *J. Amer. Chem. Soc.* **2003**, *125*, 10808.
[11] a) List, B. *J. Am. Chem. Soc.*, **2002**, *124*, 5656; a) Bogevig, A.; Juhl, K.; Kumaragurubaran, N.; Zhuang, W.; Jorgensen, K.A. *Angew. Chemie Int. Ed.,* **2002**, *41*, 1790.
[12] Pizzarello, S.; Weber, A.L. *Science* **2004**, *303*, 1151.
[13] Blackmond, D.G. *Angew. Chemie Int. Ed.,* **2005**, *44*, 4032.
[14] Girard, C.; Kagan, H.B. *Angew. Chem. Int. Ed. Engl.*, **1998,** *37*, 2907.
[15] a) List, B. *Acc. Chem. Res.*, **2004**, *37*, 548; b) List, B. *Tetrahedron* **2002**, *58*, 5573; d) Jarvo, E.R.; Miller, S.J. *Tetrahedron* **2002**, *58*, 2481; e) France, S.; Geurin, D.J.; Miller, S.J.; Lectka, T. *Chem. Rev*. **2003**, *103*, 2985.
[16] Machajewski, T.J.; Wong, C.-H. *Angew. Chemie Int. Ed.*, **2000**, *39*, 1352.
[17] a) Schreiner, P.R. *Chem. Soc. Rev.*, **2003**, *32*, 289; b) Pihko, P. *Angew. Chemie Int. Ed.*, **2004**, *43*, 2062.
[18] a) Eder, U.; Sauer, G.; Wiechert, R. *Angew. Chemie Int. Ed. Engl.* **1971**, *10*, 496; b) Hajos, Z.G.; Parrish, D.R. *J. Org. Chem.* **1974**, *39*, 1615.
[19] List, B.; Lerner, R.A.; Barbas, C.F. *J. Amer. Chem. Soc.* **2000**, *122*, 2395.
[20] a) Mathew, S.P.; Iwamura, H.; Blackmond, D.G. *Angew. Chemie Int. Ed.,* **2004,** *43*, 3317; b) Iwamura, H.; Mathew, S.P.; Blackmond, D.G. *J. Am. Chem. Soc.*, **2004**, *126*, 11770, c) Iwamura, H.; Wells, D.H. Jr.; Mathew. S.P.; Klussmann, M.P.; Armstrong, A.; Blackmond, D.G. *J. Am. Chem. Soc.*, **2004**, *126*, 13612.

Combined Reactor and Catalyst Engineering for Efficient, Decentralized Conversion of Methane to Synthesis Gas or Hydrogen

Götz Veser

Department of Chemical and Petroleum Engineering, University of Pittsburgh, Pittsburgh, PA 15261, USA

Introduction

Natural gas is receiving increasing attention as a clean(er) alternative and extension of the depleting world oil reserves. However, about half of all world natural gas reserves are currently considered as "stranded," i.e. they cannot be recovered (in an economical way) with existing technology.

At the same time, methane is a main contributor to global warming, with about 70% of all atmospheric methane of anthropogenic origin, i.e. resulting directly from human activities[1]. However, since methane has a short atmospheric lifetime (~8–12 years), it is also one of the most promising "greenhouse gases" for short-term measures to counter global warming[2]. In the United States, more than a third of all methane emissions result from landfills, which thus not only represent a significant environmental problem, but also a waste of a valuable—and renewable—resource.

In either case, the small size or remoteness of the respective methane sources does not allow exploitation with existing industrial technology. It is therefore necessary to develop new technologies for efficient small-scale and decentralized utilization of these and similar resources.

The only economic route for methane valorization, i.e. for conversion of methane into more valuable chemicals, is indirect utilization via the production of synthesis gas, a mixture of CO and hydrogen, followed by secondary processes such as methanol or Fischer-Tropsch syntheses[3]. In these processes, syngas production is currently the limiting factor with about 60% of overall investment costs. In this context, catalytic partial oxidation of methane to synthesis gas (CPOM) has recently found much attention as an alternative to the industrially dominant, highly endothermic steam reforming route. CPOM ($CH_4 + 0.5\ O_2 \rightleftharpoons CO + 2\ H_2$, $\Delta H_R = -36$ kJ/mol) is a mildly exothermic reaction and has thus the potential to be run autothermally, making it independent of external heat sources—a quintessential requirement for decentralized processes. Furthermore, the reaction is characterized by extremely high reaction rates typical for high-temperature catalytic oxidations, allowing for very short contact times in the millisecond range, and thus for extremely compact, high-throughput reactors.

However, despite its advantages over the conventional steam-reforming route, CPOM is still suffering from adiabatic equilibrium limitations and sub-optimal process yields[4, 5]. In the following we will demonstrate that by combining the CPOM reaction route with an efficient reactor concept and appropriately designed catalysts, a highly efficient and flexible syngas process for decentralized applications can be attained.

Integrated Reactor Concept: A High-Temperature Reverse-Flow Reactor (RFR). Multifunctional reactor concepts have become the subject of intense research in the last two decades, as the integration of more than one unit operation into a single reactor unit often allows significant process improvements over the conventional sequential arrangement[6-8]. A frequently used multifunctional reactor concept re-integrates the heat released by an exothermic reaction either by recuperative heat exchange in a countercurrent heat-exchange reactor[9], or, even more efficiently, by regenerative heat exchange in a reverse-flow reactor (RFR)[5].

We applied reverse-flow operation to high-temperature CPOM over a Pt-coated alumina catalyst to overcome the above-mentioned thermodynamic limitations[5, 11, 12]. The schematic reactor set-up is shown in Figure 1 (below); details on reactor set-up and operation can be found elsewhere[5]. The operational principle of the RFR becomes apparent in the time-dependent temperature profiles shown in Figure 1b: The periodic flow reversal leads to strongly increased catalyst inlet temperatures in excess of 800°C, as well as temperatures inside the catalyst zone that are increased well beyond their steady-state adiabatic limits (T>1200°C). This "super-adiabatic" operation is achieved through efficient thermal pumping of the heat reservoirs in the inert zones, as indicated by the strong spatio-temporal temperature gradients in this area (z = 10-100 mm).
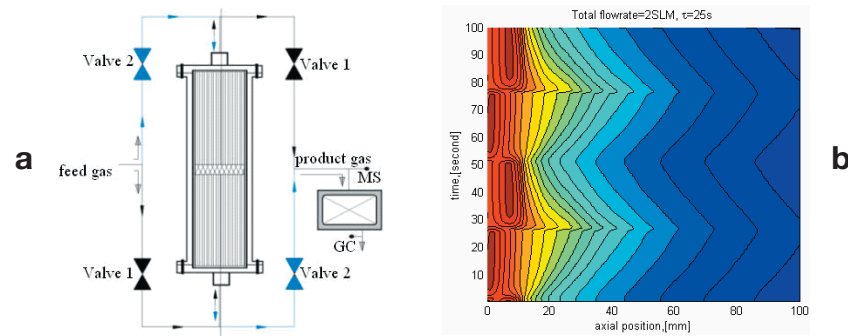

Figure 1. Left: Schematic reactor setup in the experimental RFR: a fixed-bed reactor is surrounded by four 2-way valves which are operated in synchrony to achieve periodic reversal of the flow direction in the reactor.
Right: Experimental temperature profiles in the catalyst (z=0-10mm) and one inert zone (z=10-100mm) during CPOM over a Pt/alumina catalyst ($CH_4:O_2 = 2.0$, half period $\tau = 25$ s). Two full periods at RFR operation are shown and flow direction is initially ($\tau = 0$-25 s) from left to right.

Corresponding methane conversions and hydrogen selectivities at steady-state reactor operation (SS) and at reverse-flow operation (RFR) are shown in Figure 2 as a function of methane/oxygen ratio in the feed gas. The regenerative heat integration in the RFR leads to significant improvements in methane conversion of ~20% over the whole range of conditions (left graph), as well as drastic improvements in hydrogen selectivity of up to 40% (right graph). It should be emphasized again that these improvements are achieved through no other change in the experiment than introduction of flow reversal.
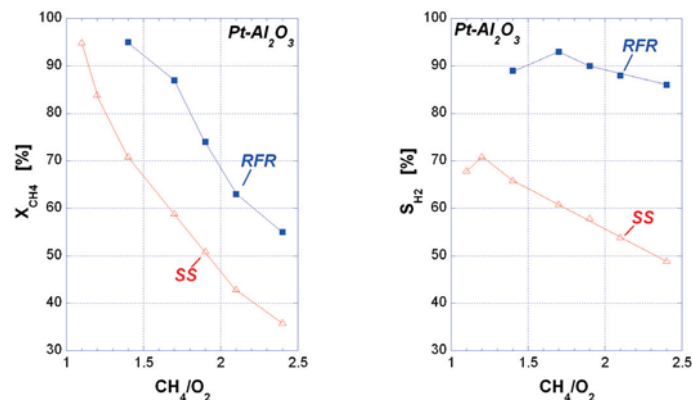
24   Contact us for bulk or custom synthesis. Visit www.strem.com for new product announcements.

info@strem.com • technical@strem.com • quotation@strem.com • order@strem.com   25

Figure 2. Experimental results for CPOM over an alumina-supported Pt catalyst in comparison between steady-state (SS) and reverse-flow operation (RFR). Methane conversions (left graph) and hydrogen selectivities (right graph) are shown versus methane/ oxygen-ratio at a reactor feed of 4 slm methane/air. The duration of one half-period at RFR operation was 15 s.

Novel Catalyst Systems: Pt-BHA Nanocomposites. As seen above, modern heat-integrated reactor concepts can achieve strongly improved processes. While these reactor concepts can (partially) compensate for poor catalyst selectivity or activity[12], modern reaction engineering needs to combine reactor engineering with the design of suitably adapted catalyst systems to harvest the full potential of modern reactor concepts.

We therefore developed a novel synthesis for the design of highly active, selective, and high-temperature stable catalysts for this reaction system. The synthesis route is based on the simultaneous synthesis of a ceramic matrix (here: a barium-hexaaluminate, or BHA) and metal nanoparticles (here: platinum), using a microemulsion-templated sol-gel route (for experimental details, see [13-16]). The synthesis yields a fine nanocomposite powder which consists of loose agglomerates of nanoparticles with a highly uniform distribution of Pt nanoparticles in a matrix of ceramic particles (see Figure 3a).
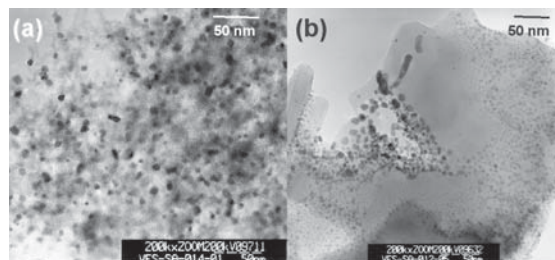
Figure 3. Nanocomposite Pt-BHA catalyst (at left) in comparison to a BHA support impregnated via conventional methods with a Pt-salt (right), both after 5h calcination in air at 600°C. One can clearly see a strongly improved uniformity in size distribution as well as in spatial distribution of the Pt-nanoparticles in the nanocomposite catalyst.

These new nanocomposites were tested in CPOM. Results at steady-state reactor operation are shown in Figure 4 (open triangles and dotted lines). Strong improvements by ~20% in methane conversion and by 10-30% in hydrogen selectivity are achieved in comparison to a conventional alumina supported Pt catalyst (compare to open triangles and dotted lines in Figure 2). Most significantly, while conventional catalysts suffer from deactivation at the extreme high-temperature conditions of CPOM, the novel nanocomposite is stable with no deactivation or sintering detectable during extended reactor operation[15, 17], making them particularly promising for application at the extremely harsh conditions of RFR operation.

Combining Reactor Concept and Catalyst System: Pt-BHA in RFR. Since both the integrated reactor concept and the novel catalysts each lead to strong improvements in hydrogen yields (as well as CO yields, not shown in these figures), we tested the application of the nanocomposite catalyst to RFR operation. Results are shown by the filled square and solid lines in Figure 4. Clearly, RFR operation with the nanocomposite leads to a further improvement in conversion and selectivity, surpassing both the steady-state nanocomposite (open symbols and dotted lines in Figure 4) as well as the RFR with a conventional catalyst (Figure 2, filled symbols and solid lines). The combination of the integrated reactor concept with novel, high-temperature stable nanocomposites results in methane conversion at stoichiometric conditions of ~80% with hydrogen selectivities of ~95%, a drastic improvement in comparison to < 50% conversion and ~55% H_2 selectivity with a conventional catalyst at conventional reactor operation. In fact, syngas yields for the combined nanocatalyst/RFR system compare quite favorably with yields in modern steam reforming plants—although the presented results were achieved in a radically more simple process with highly compact reactors at autothermal operation with air!
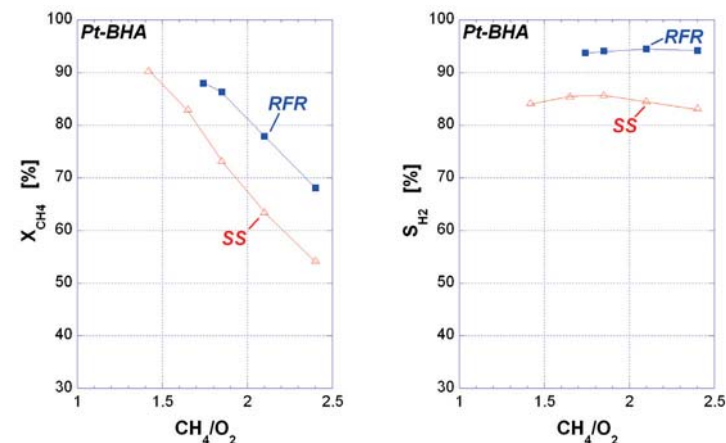

Figure 4. Experimental results for CPOM over a novel nanocomposite Pt-BHA catalyst in a comparison between steady-state (SS) and reverse-flow operation (RFR). Methane conversions (left graph) and hydrogen selectivities (right graph) are shown versus methane/oxygen-ratio at a reactor feed of 4 slm methane/ air. The duration of one half-period at RFR operation was 15 s.

Conclusions

We presented some recent results from our ongoing studies towards the development of a flexible and efficient process for methane valorization via direct catalytic partial oxidation to synthesis gas or hydrogen. We aimed to demonstrate that the combination of modern reactor engineering with the emerging nanoengineering of catalyst systems can open new frontiers even for well-studied and well-established chemical processes. This combination of reactor and catalyst engineering is essential for the development of novel and improved processes that we see as critical enabling technologies for a more efficient and sustainable future.

References

[1] IPCC report "Climate Change 2001: The Scientific Basis," 2001.
[2] Hansen, J.; Sato, M.; Ruedy, R.; Lacis, A.; Oinas, V. *Proc. Natl. Acad. Sci.* **2000**, *97*, 9875.
[3] Wender, I. *Fuel Proc. Technol.* **1996**, *48*, 189.
[4] Neumann, D.; Veser, G. *ACS Fuel Preprints* **2003**, *48*, 224.
[5] Neumann, D.; Veser, G. *AIChE J.* **2005**, *51*, 210.
[6] Agar, D. W. *Chem. Eng. Sci.* **1999**, *54*, 1299.
[7] Kolios, G.; Frauhammer, J.; Eigenberger, G. *Chem. Eng. Sci.* **2000**, *55*, 5945.
[8] Westerterp, K. R. *Chem. Eng. Sci.* **1992**, *47*, 9.
[9] Friedle, U.; Veser, G. *Chem. Eng. Sci.* **1999**, *54*, 1325.
[10] Eigenberger, G.; Nieken, U. *Intl Chem. Eng.* **1994**, *34*, 4.
[11] Neumann, D.; Gepert, V.; Veser, G. *Ind. & Eng. Chem. Res.* **2004**, *43*, 4657.
[12] Mitri, A.; Neumann, D.; Liu, T. F.; Veser, G. *Chem. Eng. Sci.* **2004**, *59*, 5527.
[13] Kirchhoff, M.; Specht, U.; Veser, G. In *NSTI Nanotechnology 2004*: Boston, 2004; p. 268.
[14] Kirchhoff, M.; Specht, U.; Veser, G. In *Solid State Ionics 2002*; Knauth, P., Ed.; MRS Publishing, 2002; p. 891.
[15] Kirchhoff, M.; Specht, U.; Veser, G. *Nanotechnology* **2005**, *16*, S401.
[16] Kirchhoff, M.; Specht, U.; Veser, G. In *Innovation in the Manufacture and Use of Hydrogen*; Emig, G., Ed.; DGMK Publishing: Hamburg, 2003; p. 33..
[17] Schicks, J.; Neumann, D.; Specht, U.; Veser, G. *Catal. Today* **2003**, *83*, 287.

Palladium-Catalyzed 4-Component Coupling to Give β-Selenyl Acrylamides

Tara Y. Meyer and Daniel J. Knapton
Department of Chemistry
University of Pittsburgh
Pittsburgh, PA 15261 USA

Catalysis is an area of research that has long attracted the attention of both chemists and chemical engineers. Moreover, it is an area to which Professor Irving Wender has contributed enormously. As a member of a younger generation who has benefited from his pioneering efforts, I feel privileged to discuss in his 90th birthday symposium our own recent efforts in catalysis. Specifically, I will describe a palladium mediated Multi-Component Coupling (MCC) to give β-selenyl acrylamides that has been developed in my laboratory by my former Ph.D. student, Dr. Daniel Knapton (Scheme 1).[1, 2]

Scheme 1
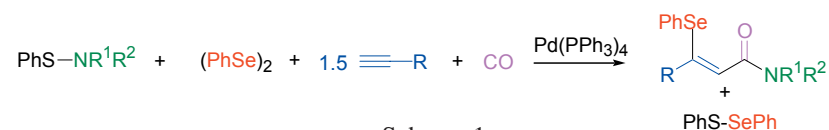
Before beginning, it is useful to review the advantages of MCC reactions. The classic approach to the synthesis of complex molecules involves sequences of bimolecular reactions. After each step, intermediates are isolated and purified. Even with reasonable yields for the individual steps, the overall yield drops significantly as you proceed through the synthesis. MCC's, in contrast, involve a single pot combination of multiple reagents. This method reduces purification time, increases yield and, if substituents can be varied on the components, invites combinatorial strategies.[3, 4]

The class of compounds that we are targeting is the β-selenyl acrylamides. These molecules are potentially useful synthons for more elaborate products because they bear two transformable functional groups. The phenylselenyl groups are pseudo halides that can be replaced or modified in a variety of ways.[5] Also present is the extremely useful α,β-unsaturated moiety which can participate in a variety of additions and cyclizations.

The four components of the synthesis are a sulfenamide, diphenyl diselenide, alkyne and CO (Scheme 1). In the presence of 4 mol% Pd(PPh$_3$)$_4$, these components combine to give the β-selenyl acrylamide product and an equivalent of the mixed diphenyl dichalcogenide, PhSe-SPh. The reaction is stereospecific and regioselective; the selenyl group is always *cis* relative to the carbonyl and the amide functional group is directed to the less substituted end of the alkyne.

The products are obtained in good to excellent yields (65-95% relative to sulfenamide) and the reaction is reasonably general, tolerating a range of substituents on the nitrogen and the alkyne. The nitrogen can bear dimethyl, diethyl, methyl benzyl, allyl methyl and diallyl subtituents. The alkyne can bear a variety of terminal groups including Cl, OAc, NR$_2$, CN and Ph.

28   Contact us for bulk or custom synthesis. Visit www.strem.com for new product announcements.

info@strem.com • technical@strem.com • quotation@strem.com • order@strem.com   29

Based on a detailed study of the 2- and 3-component side-products from this reaction and the relevant precedents[6-8], we propose the following catalytic cycle (Scheme 2). The central pathway involves the initial addition of diphenyl diselenide to form the bis(phenylselenato) palladium (I). Insertion of alkyne gives a vinyl intermediate (IV). Subsequent insertion of CO produces the acyl (VI). Nucleophilic attack by sulfenamide can then give the product (IX). A palladium complex bearing at least one phenylthio group is produced concurrently. Alkyne insertion can, of course, proceed directly from this point (VI). Alternatively, reductive elimination can lead back to the unsaturated palladium complex at the beginning of the cycle (XI). It is obvious that after a few turnovers, sulfur will be introduced into the product. It also is important to note that the major side products produced can be accounted for in the catalytic cycle. Two of these products, the chalcogenyl carbamate and the chalcogenyl ester, can also directly participate in the formation of the β-selenyl acrylamide (III, X and VIII).
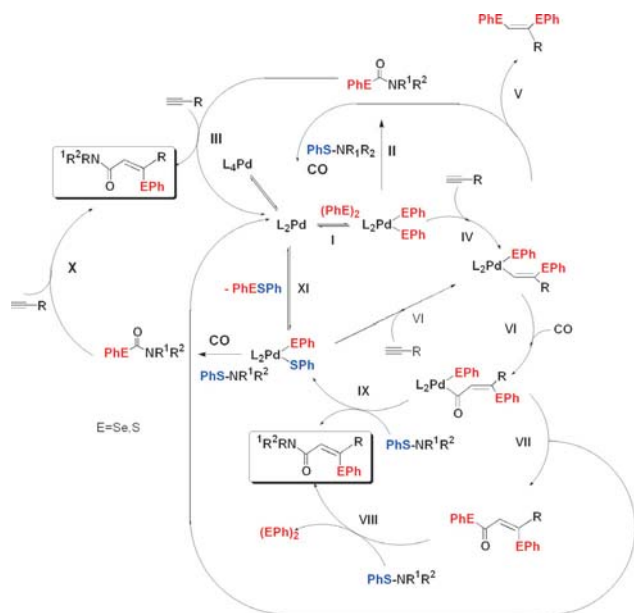
Scheme 2

The degree of sulfur incorporation is a key topic of interest. Despite the reaction stoichiometry, which employs a 2:1 ratio of Se to S, β-selenyl product is isolated in a 7:1 ratio over the analogous β-phenylthio derivative. Control experiments determined that the CO insertion step is responsible for the selectivity. When examining the 3-component carbonylative addition reaction at low CO pressures, a striking difference in the tendency for CO insertion was observed between selenium and sulfur. The sulfur derivative was extremely unreactive at low CO pressures (Scheme 3). As increasing CO pressure does increase the yield of the thioester product, it appears as if the equilibrium for CO insertion favors the formation of acyl species in the case of selenium but does not in the case of sulfur.
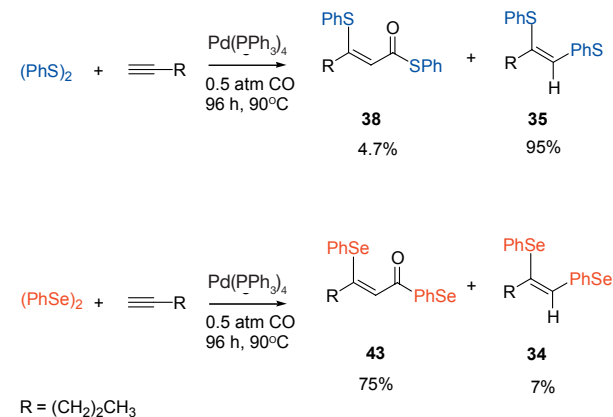
Scheme 3

Chelation likely plays a role in this phenomenon. Either the chelation of the selenium in the vinyl precursor promotes CO insertion or the chelation of the CO in the acyl product disfavors CO deinsertion. We have not yet had the opportunity to test this theory. It is known, however, that selenoethers coordinate more strongly than thioethers to palladium (II) species.[9]
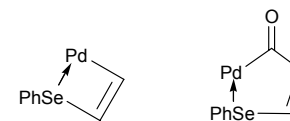
Scheme 4

Finally, selectivity also depends on the degree of conversion. When examined early in the reaction (< 50% conversion), the selectivity was as high as 12:1 in favor of selenium. After ~24 h, the selectivity drops to the generally observed 7:1 ratio. This observation is not surprising since, early in the reaction, there simply is no diphenyl disulfide or mixed dichalcogenide (PhS-SePh) present in the reaction mixture. Only after a few times through the cycle would one expect to start seeing the buildup of sulfur-containing intermediates such that they could begin to participate in the catalytic cycle.

In conclusion, we report the development of a new 4-component coupling for the production of the useful synthetic intermediates, β-selenyl acrylamides. Mechanistic studies determined that the CO insertion step is the primary contributor to the observed selectivity for selenium vs. sulfur in the β-position.

References
[1] Knapton, D. J.; Meyer, T. Y. *Org. Lett.* **2004**, *6*, 687-689.
[2] Knapton, D. J.; Meyer, T. Y. *J. Org. Chem* **2005**, *70*, 785-796.
[3] Armstrong, R. W.; Combs, A. P.; Tempest, P. A.; Brown, S. D.; Keating, T. A. *Acc. Chem. Res.* **1996**, *29*, 123-131.
[4] Weber, L.; Illgen, K.; Almstetter, M. *Synlett* **1999**, 366-374.

30   Contact us for bulk or custom synthesis. Visit www.strem.com for new product announcements.

info@strem.com • technical@strem.com • quotation@strem.com • order@strem.com   31

[5] Comasseto, J. V.; Ling, L. W.; Petragnani, N.; Stefani, H. A. *Synthesis* **1997**, 373-403.

[6] Kuniyasu, H.; Ogawa, A.; Miyazaki, S. I.; Ryu, I.; Kambe, N.; Sonoda, N. *J. Am. Chem. Soc.* **1991**, *113*, 9796-9803.

[7] Ananikov, V. P.; Beletskaya, I. P. *Dokl. Chem.* **2003**, *389*, 81-86.

[8] Kuniyasu, H.; Hiraike, H.; Morita, M.; Tanaka, A.; Sugoh, K.; Kurosawa, H. *J. Org. Chem.* **1999**, *64*, 7305-7308.

[9] Levason, W.; Orchard, S. D.; Reid, G. *Coord. Chem. Rev.* **2002**, *225*, 159-199.

New Products Introduced Since The Strem Chemiker Vol. XXI

METAL CATALYSTS FOR ORGANIC SYNTHESIS

COPPER

29-4000 Bromo(1,10-phenanthroline)(triphenyl-phosphine)copper (I), 98% *[25753-84-8]* $CuBr(C_{12}H_8N_2)P(C_6H_5)_3$; FW: 595.94; yellow pwdr.

1g
5g
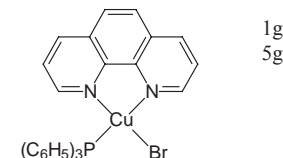
Technical Notes:
1. High yield synthesis of diarylacetylenes via the copper (I) catalyzed coupling of aryl iodides and phenylacetylene.
2. High yield synthesis of 1,3-enynes via the copper(I) catalyzed coupling of vinyl iodides and phenylacetylene.

Tech. Note (1)
Ref. (1)

80-97%

Tech. Note (2)
Ref. (2)

81-99%
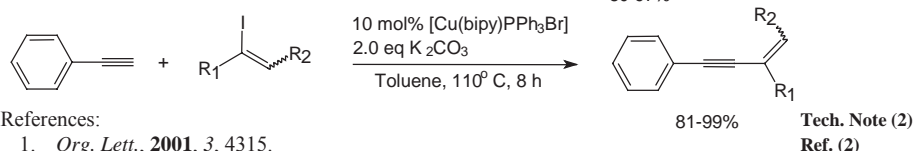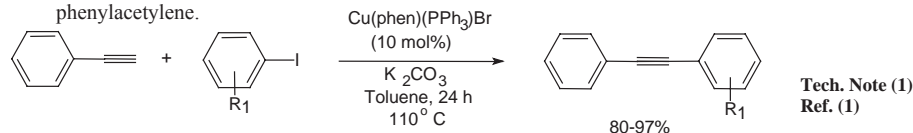
References:
1. *Org. Lett.*, **2001**, *3*, 4315.
2. *Org. Lett.*, **2004**, *6*, 1441.

29-6000 (1,10-Phenanthroline)bis(triphenyl-phosphine)copper (I) nitrate dichloro-methane adduct, 98% *[33989-10-5]* $[Cu(C_{12}H_8N_2)[P(C_6H_5)_3]_2]^+NO_3^- 1/2CH_2Cl_2$; FW: 830.33 (872.80); yellow pwdr.

5g
25g
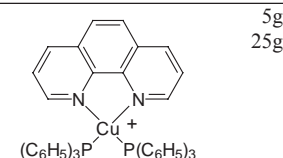
Technical Note:
1. High yield synthesis of 2-arylbenzo[*b*]furans via the copper (I) catalyzed coupling of o-iodophenols and aryl acetylenes.
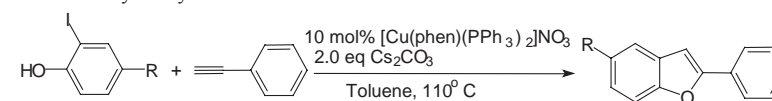
Reference:
1. *Org. Lett.*, **2002**, *4*, 4727.

IRON

26-0246 (S,S)-(-)-2,2'-Bis[(R)-(N,N-dimethyl-amino)(phenyl)methyl]-1,1'-bis(di(3,5-dimethylphenyl)phosphino) ferrocene, min. 97% *[793718-16-8]* $C_{60}H_{66}FeN_2P_2$; FW: 932.99; orange pwdr.

100mg
500mg

Note: Sold in collaboration with Solvias for research purposes only. Solvias MandyPhos™ Ligand Kit component.

Technical Note:
1. See 26-0240 (Catalog 20 page 353).

32   Contact us for bulk or custom synthesis. Visit www.strem.com for new product announcements.

info@strem.com • technical@strem.com • quotation@strem.com • order@strem.com   33

IRON (cont.)

26-0254 (S,S)-(-)-2,2'-Bis[(R)-(N,N)-dimethyl-amino)(phenyl)methyl]-1,1'-bis(di(2-methylphenyl)phosphino)ferrocene, min. 97% [831226-37-0]
$C_{56}H_{58}FeN_2P_2$; FW: 876.88; $[\alpha]_D$ −196° orange pwdr.

100mg
500mg

Note: Sold in collaboration with Solvias for research purposes only. Solvias MandyPhos™ Ligand Kit component.
Technical Note:
1. See 26-0240 (Catalog 20 page 353).

26-1153 (S)-(-)-[(S)-2-Diphenylphosphino-ferrocenyl][2-bis(3,5-dimethyl-4-methoxyphenyl)phosphino-phenyl]methanol, min. 97% [851308-47-9]
$C_{47}H_{47}FeO_2P_2$; FW: 777.68; orange foam; $[\alpha]_D$ −32° (c 0.5,CHCl$_3$)

100mg
500mg

Note: Sold in collaboration with Solvias for research purposes only.

26-1160 (S)-(-)-[(S)-2-Diphenylphosphinoferrocenyl][2-diphenylphosphinophenyl]methanol, min. 97% [851308-43-5]
$C_{41}H_{34}FeOP_2$; FW: 660.50; yellow pwdr.; $[\alpha]_D$ −70° (c 0.5, CHCl$_3$)

100mg
500mg

Note: Sold in collaboration with Solvias for research purposes only.

26-1560 (S)-(-)-[(S)-2-Di(3,5-xylyl)phosphino-ferrocenyl][2-di(4-trifluoromethyl-phenyl)phosphinophenyl]methanol, min. 97% [851308-48-0]
$C_{47}H_{40}F_6FeOP_2$; FW: 852.60; yellow pwdr.; $[\alpha]_D$ −44° (c 0.5, CHCl$_3$)

100mg
500mg

Note: Sold in collaboration with Solvias for research purposes only.

26-1565 (S)-(-)-[(S)-2-Di(3,5-xylyl)phosphino-ferrocenyl][2-di(3,5-xylyl)phosphino-phenyl]methanol, min. 97% [851308-45-7]
$C_{49}H_{50}FeOP_2$; FW: 772.71; orange foam; $[\alpha]_D$ −51° (c 0.5,CHCl$_3$)

100mg
500mg

Note: Sold in collaboration with Solvias for research purposes only.

GOLD

79-5000 Methyl(triphenylphosphine)gold (I), 99% [23108-72-7]
Au(CH$_3$)P(C$_6$H$_5$)$_3$; FW: 474.29; white xtl.; m.p. 150° (dec.)

250mg
1g

Technical Notes:
1. Catalyst used for the addition of water to akynes.
2. Highly efficient catalyst for the intermolecular hydroamination of alkynes.

Tech. Note (1)
Ref. (1)

Tech. Note (1)
Ref. (2)
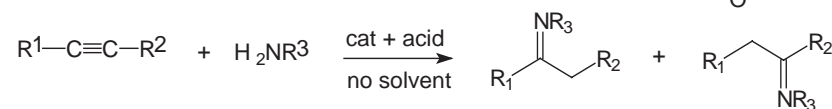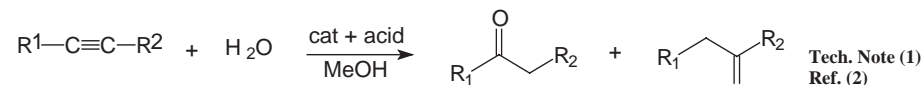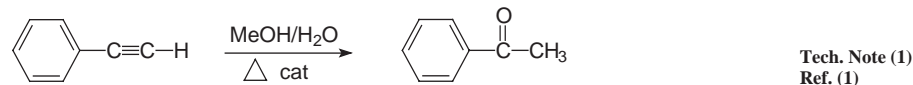
Tech. Note (2)
Ref. (3)

References:
1. *J. Am. Chem. Soc.*, **2003**, *125*, 11925.
2. *Angew. Chem. Int. Ed.*, **2002**, *41*, 4563.
3. *Org. Lett.*, **2003**, *5*, 3349.

IRIDIUM

77-0500 Chlorodihydrido[bis(2-di-i-propylphosphino-ethyl)amine]iridium (III), min. 98% [791629-96-4]
IrClH$_2$(C$_{16}$H$_{37}$NP$_2$); FW: 535.10; white pwdr.

250mg
1g

Note: Sold under license from Kanata for research purposes only. Patents WO04096735; US 10/985,058.
Technical Note:
1. Catalyst used for transfer hydrogenation.
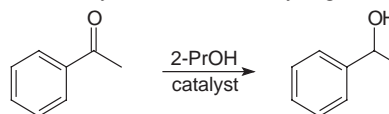
Reference:
1. Patent WO 2004096735.

LITHIUM

03-2010 Lithium tris(S-(-)-1,1'-binaphthyl-2,2'-diolato)yttrate (III), min. 97% [500995-67-5]
3Li$^+$[(C$_{20}$H$_{12}$O$_2$)$_3$Y]$^{3-}$; FW: 962.65; white pwdr.

250mg
1g
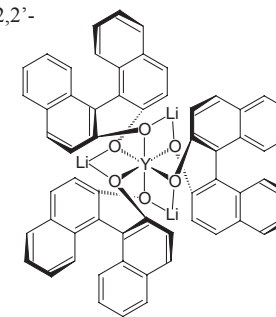
LITHIUM (cont.)

03-2010 (cont.) Lithium tris(S-(-)-1,1'-binaphthyl-2,2'-diolato)yttrate (III), min. 97%
[500995-67-5]

Technical Notes:
1. Catalyst used for the asymmetric cyano-ethoxycarbonylation reaction of aldehydes.
2. Catalyst used for the efficient, two-step conversion of α,β-unsaturated aldehydes to optically active γ-oxy-α,β-unsaturated nitriles.
3. Catalyst used for the asymmetric 1,4-addition of O-alkylhydroxyamine to enones.

Tech. Note (1)
Ref. (1)

Tech. Note (2)
Ref. (2)

Tech. Note (3)
Ref. (3)
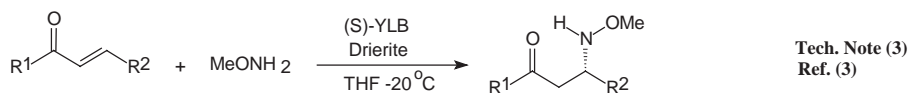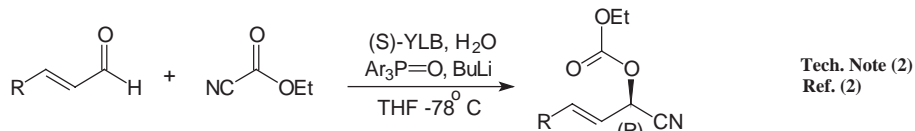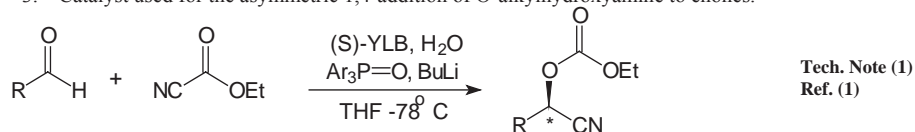
References:
1. *J. Am. Chem. Soc.*, **2005**, *127*, 3413.
2. *Org. Lett.*, **2003**, *5*, 3021.
3. *J. Am. Chem. Soc.*, **2003**, *125*, 16178.

PALLADIUM

46-0039 Allylchloro[1,3-bis(2,6-di-i-propyl-phenyl)-4,5-dihydroimidazol-2-ylidene] palladium (II), 97% [478980-01-7]
$C_{30}H_{43}ClN_2Pd$; FW: 573.55; white pwdr.   250mg / 1g

Technical Note:
1. Catalyst used for the cross-coupling of aryl chlorides with amines, boronic acids and ketones.

1 mol% Pd catalyst
t-Bu ONa
RT   Ref. (1)

1 mol% Pd catalyst
t-Bu ONa
THF, 50-70°, 1-4 hr   Ref. (2)
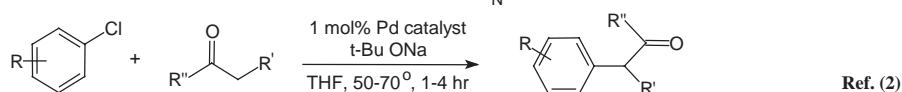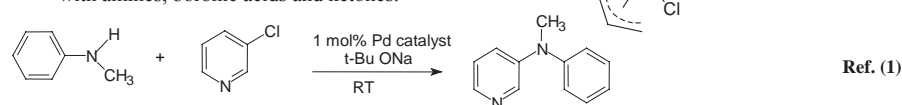
References:
1. *Organometallics*, **2002**, *21*, 5470.
2. *Org. Lett.*, **2002**, *4*, 4053.

PHOSPHORUS

96-6651 Degussa cataCXium® Ligand Kit for C-X coupling reactions   1 kit
Contains the following:

15-0038	1g	15-3550	500mg
15-0483	1g	15-3600	500mg
15-1807	500mg	15-3605	500mg
15-1808	500mg	15-3610	500mg
15-2975	500mg	46-0290	1g
15-2980	500mg		

PHOSPHORUS (cont.)

15-0106 (S,S)-(+)-1,2-Bis{(S)-4,5-dihydro-3H-binaphtho[1,2-c:2',1'-e] phosphepino}benzene, 97% (S)-BINAPHANE   100mg / 500mg
$C_{50}H_{36}P_2$; FW: 698.77; light yellow pwdr.
air sensitive

Note: Sold in collaboration with Chiral Quest for research purposes only. US Patent 6,525,210.
Technical Note:
1. See 15-0103 (Catalog 20 page 397).

15-0108 (-)-2,3-Bis[(2R,5R)-2,5-dimethylphospholanyl] maleic anhydride, min. 97% [catASium® M(R)]   100mg / 500mg
[505092-86-4]
$C_{16}H_{24}O_3P_2$; FW: 326.31; brown pwdr.
air sensitive
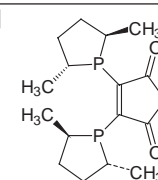
Note: Degussa catASium® M Toolbox Kit component.
Sold in collaboration with Degussa for research purposes only. Patent WO03084971.
Technical Note:
1. See 45-0173 (Catalog 20 page 451).

15-0176 (S)-(+)-1,13-Bis(diphenylphosphino)-7,8-dihydro-6H-dibenzo[f,h][1,5]dioxonin, 95% (S)-C_3-TUNEPHOS   100mg / 500mg
[486429-99-6]
$C_{39}H_{32}O_2P_2$; FW: 594.62; white pwdr.
air sensitive

Note: Sold in collaboration with Chiral Quest for research purposes only. US Patent No. 6,521,769.
Additional patents pending.
Technical Note:
1. See 15-0175 (Catalog 20 page 408).

15-0473 (-)-1,2-Bis((2R,5R)-2,5-diphenyl-phospholano)ethane, min. 98% (R,R)-Ph-BPE [528565-79-9]   100mg / 500mg / 2g
$(C_{16}H_{16})PCH_2CH_2P(C_{16}H_{16})$;
FW: 506.60; white solid; m.p. 144°;
$[\alpha]_D$ −182.7° (c 1.0, CH_2Cl_2)
air sensitive
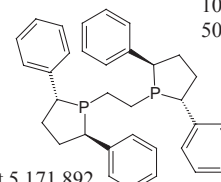
Note: Manufactured under US Patent 5,021,131 and US Patent 5,171,892.
Technical Notes:
1. Phenyl-BPE exhibits enhanced activity and selectivity over existing members of the BPE ligand family in rhodium catalysed asymmetric hydrogenation.
2. This ligand is highly efficient for the hydrogenation of N-acyl aryl-enamides.
3. Molar substrate/catalyst ratios of up to 100,000/1 are achieved with excellent reactivity and enantioselectivity using commercial grade substrates and solvents.

[(R,R)-Ph-BPE Rh (COD)]BF₄
S/C 100,000
10 bar H₂, MeOH, 25° C

100% conversion
99% ee   Ref. (1)

[(R,R)-Ph-BPE Rh (COD)]BF₄
S/C 3000
10 bar H₂, MeOH, 28° C

100% conversion
99% ee   Ref. (1)
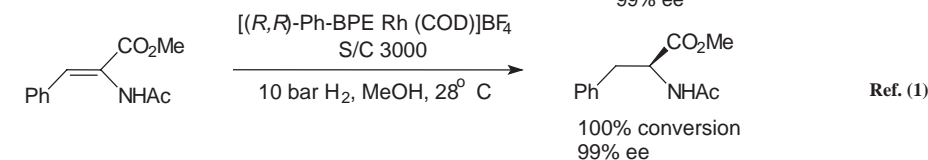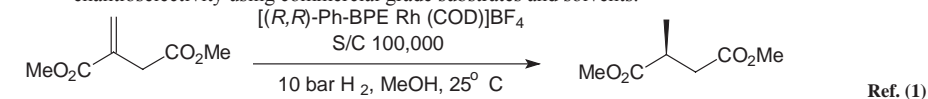
PHOSPHORUS (cont.)

15-0473 (-)-1,2-Bis((2R,5R)-2,5-diphenylphospholano)ethane, min. 98% (R,R)-Ph-BPE
(cont.) *[528565-79-9]*

[(S,S)-Ph-BPE Rh (COD)]BF₄
S/C 5000-1000

10 bar H₂, MeOH, 25° C

Ref. (2)

98-99% ee
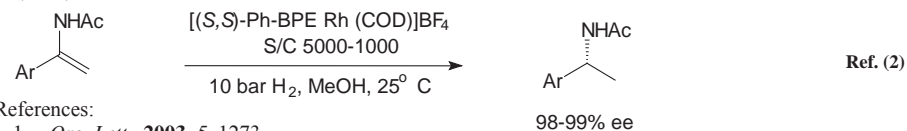
References:
1. *Org. Lett.*, **2003**, *5*, 1273.
2. *Tetrahedron Lett.*, **2004**, *45*, 9277.

15-0474 (+)-1,2-Bis((2S,5S)-2,5-diphenylphospholano)ethane,   100mg
min. 98% (S,S)-Ph-BPE *[824395-67-7]*   500mg
(C₁₆H₁₆)PCH₂CH₂P(C₁₆H₁₆); FW: 506.60; white solid;   2g
m.p. 144 °; [α]$_D$ +182.7° (c 1.0, CH₂Cl₂)
air sensitive

Note: Manufactured under US Patent 5,021,131 and US Patent 5,171,892.
Technical Note:
1. See 15-0473 (page 37).

15-1060 (1R,1'R,2S,2'S)-(+)-2,2'-Di-t-butyl-2,3,2',3'-   100mg
tetrahydro-1,1'-bi-1H-isophosphindole,   500mg
min. 98% (R,R,S,S)-DUANPHOS
C₂₄H₃₂P₂; FW: 382.46; white xtl.; [α]$_D$ +19.5
air sensitive

Note: Sold in collaboration with Chiral Quest for research purposes only. Patent pending, PCT/US02/35788.
Technical Note:
1. As a highly electron-donating and conformationally rigid ligand, the rhodium complex of DuanPhos has exhibited remarkably high enantioselectivities and reactivities for the hydrogenation of a variety of functionalized olefins.

Rh-duanphos complex

MeOH, K₂CO₃, H₂ (10 bar), 50 °C

yields >90%
up to > 99% ee
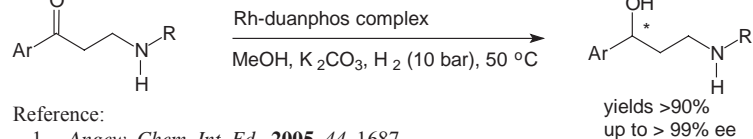
Reference:
1. *Angew. Chem. Int. Ed.*, **2005**, *44*, 1687.

15-1142 2'-Dicyclohexylphosphino-2,6-dimethoxy-3-   500mg
sulfonato-1,1'-biphenyl hydrate sodium salt,   2g
min. 98%
C₂₆H₃₄NaO₅PS·XH₂O;
FW: 512.58; light yellow solid

Note: Soluble version of 15-1143 S-Phos. Buchwald Biaryl Phosphine Ligand Kit component. Patents: US 6,395,916, US 6,307,087.
Technical Note:
1. The first general catalysts for the Suzuki-Miyaura and Sonogashira coupling of aryl chlorides and for the coupling of challenging substrate combinations in water.
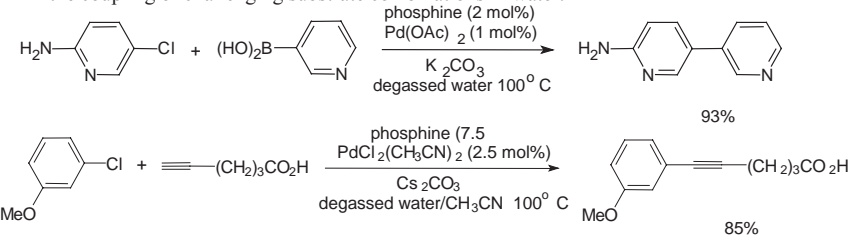
phosphine (2 mol%)
Pd(OAc)₂ (1 mol%)

K₂CO₃
degassed water 100° C

93%

phosphine (7.5
PdCl₂(CH₃CN)₂ (2.5 mol%)

Cs₂CO₃
degassed water/CH₃CN 100° C

85%

Reference:
1. *Angew. Chem. Int. Ed.*, **2005**, *44*, 6173.

PHOSPHORUS (cont.)

15-1146 2-Dicyclohexylphosphino-2',6'-di-i-propoxy-1,1'-   500mg
biphenyl, min. 98% RuPhos *[787618-22-8]*   2g
C₃₀H₄₃O₂P; FW: 466.64; white pwdr.;
m.p. 123-124°

Note: Buchwald Biaryl Phosphine Ligand Kit component.
Patents: US 6,395,916, US 6,307,087.
Technical Note:
1. An extremely active catalyst for the Negishi Cross-coupling reaction.

Pd₂dba₃
15-1146

THF
70° C, 15h

(Ligand:Pd=2:1)

Pd₂dba₃
15-1146

THF
70° C, 15h

(Ligand:Pd=2:1)
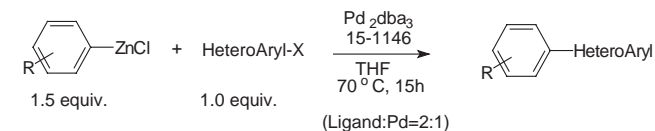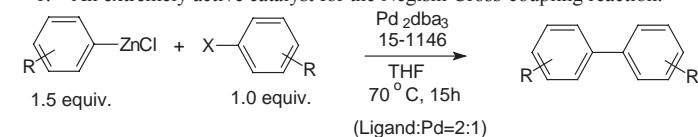
Reference:
1. *J. Am. Chem. Soc.*, **2004**, *126*, 13028.

15-1452 (1R)-(+)-3-[Di(3,5-dimethylphenyl)phosphino]-   100mg
2-(4-diphenylphosphino-2,5-dimethylthien-   500mg
3-yl)-1,7,7-trimethylbicyclo[2.2.1]hept-
2-ene, min. 98% [catASium® T2]
C₄₄H₄₈P₂S; FW: 670.87; white to
yellow pwdr.; [α]$_D$ +99.1 (c 1.0, CHCl₃)
air sensitive

Note: Optical purity 97+%.
Technical Note:
1. Highly enantioselective catalyst for the hydrogenation of α- and β-acylamido acrylates or less functionalized olefins under mild conditions.

[Rh(COD)L]BF₄

0.1 mol% catalyst
toluene, 3bar H₂
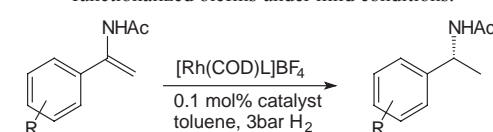
Reference:
1. Submitted.

15-1241 9,9-Dimethyl-4,5-bis(di-t-butylphosphino)   500mg
xanthene, min. 97% t-Bu-XANTPHOS   2g
C₃₁H₄₈OP₂; FW: 498.66;
white to light yellow pwdr.

Technical Note:
1. See 15-1242 (Catalog 20 page 429).

15-1455 6,6'-[[(1R,3R)-1,3-Dimethyl-1,3-propane-   100mg
diyl]bis(oxy)]bis[4,8-bis(t-butyl)-2,10-   500mg
dimethoxy-bibenzo[d,f][1,3,2]dioxa-
phosphepin, min. 95%
(R,R)-Chiraphite
[149646-83-3]
C₄₉H₆₆O₁₀P₂; FW: 876.99;
off-white pwdr.
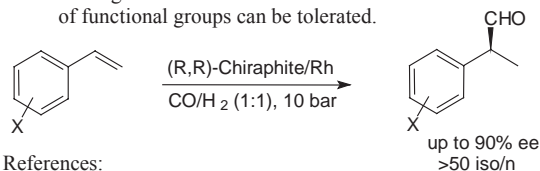*air sensitive, moisture sensitive*

PHOSPHORUS (cont.)

15-1455   6,6'-[[(1R,3R)-1,3-Dimethyl-1,3-propanediyl]bis(oxy)]bis[4,8-bis(t-butyl)-2,10-dimethoxy-bibenzo[d,f][1,3,2]dioxaphosphepin, min. 95% (R,R)-Chiraphite [149646-83-3]

Note: Sold in collaboration with Chirotech for research purposes only. US Patent No. 5,491,266.

Technical Note:

1. Useful catalyst for the asymmetric hydroformylation of olefins under mild conditions. High enantio- and regioselectivities have been demonstrated for several prochiral vinylarenes, and a wide variety of functional groups can be tolerated.

References:

1. *J. Org. Chem.*, **2004**, *69*, 4031.
2. *Organometallics*, **1997**, *16*, 2929.
3. *J. Chem. Soc.*, Dalton Trans., **1995**, 409.

15-1456   6,6'-[[(1S,3S)-1,3-Dimethyl-1,3-propanediyl]bis(oxy)] bis[4,8-bis(t-butyl)-2,10-dimethoxy-bibenzo[d,f][1,3,2] dioxaphosphepin, min. 95% (S,S)-Chiraphite $C_{49}H_{66}O_{10}P_2$; FW: 876.99; off-white pwdr.   100mg 500mg
air sensitive, moisture sensitive

Note: Sold in collaboration with Chirotech for research purposes only. US Patent No. 5,491,266.

Technical Note:

1. See 15-1455 (page 39).

15-1238   [(1R,2R,3S)-(+)-1,2-Dimethyl-2,3-bis(diphenylphosphinomethyl) cyclopentyl]methanol, min. 90% [catASium® I] [497262-02-9] $C_{34}H_{38}OP_2$; FW: 524.61; colorless, viscid oil; [α]$_D$ +66.8° (c 1,CHCl$_3$)   100mg 500mg
air sensitive
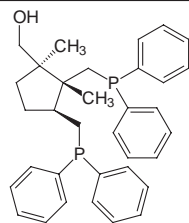
Note: Sold in collaboration with Degussa for research purposes only. Patent No. WO 2003099832.

Technical Note:

1. Highly enantioselective catalyst for the hydrogenation of α-acylamido acrylates and E or Z β-acylamido acrylates under mild conditions and low pressure.
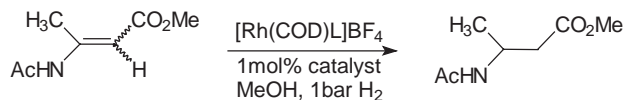
Reference:

1. Tetrahedron: *Asymmetry*, **2002,** *13,* 1615.

15-1807   Di-(2-pyridyl)(dicyclohexylphosphino) amine, min. 94% [cataCXium® KCy] [472959-98-1] $C_{22}H_{30}N_3P$; FW: 367.47; white to yellow pwdr.   500mg 2g
air sensitive
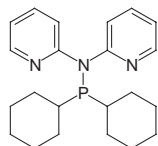
Note: Sold in collaboration with Degussa for research purposes only. Patent WO 0343735.

Technical Note:

1. Useful ligand for the palladium-catalyzed Suzuki coupling reaction using aryl chlorides.

Reference:

1. *Angew. Chem. Int. Ed.*, **2002**, *41(9)*, 1521.

PHOSPHORUS (cont.)

15-1808   Di-(2-pyridyl)(diphenylphosphino)amine, min. 96% [cataCXium® KPh] [472959-76-5] $C_{22}H_{18}N_3P$; FW: 355.37; white to yellow pwdr.   500mg 2g
air sensitive
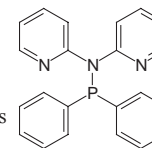
Note: Sold in collaboration with Degussa for research purposes only. Patent WO 0343735.

Technical Note:

1. See 15-3550.

15-2975   N-(2-Methoxyphenyl)-2-(di-t-butylphosphino) pyrrole, min. 92% [cataCXium® POMetB] $C_{19}H_{28}NOP$; FW: 317.41; white to yellowish pwdr.   500mg 2g
air sensitive
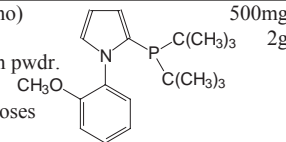
Note: Sold in collaboration with Degussa for research purposes only. Patent Application pending.

Technical Note:

1. See 15-3550 (page 41).

15-3550   N-Phenyl-2-(di-t-butylphosphino)indol, min. 96% [cataCXium® PIntB] $C_{26}H_{37}NP$; FW: 394.55; white to yellow pwdr.   500mg 2g
air sensitive
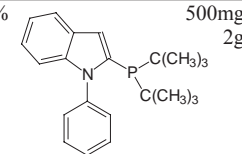
Note: Sold in collaboration with Degussa for research purposes only. Patent Application pending.
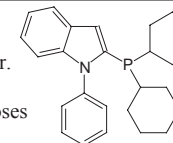
Technical Note:

1. Useful ligand for the Pd-catalyzed amination reaction.
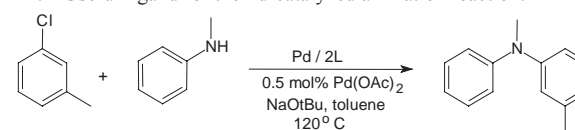
Reference:

1. *Chemistry European Journal*, **2004**, *10*, 2983.

15-3605   N-Phenyl-2-(dicyclohexylphosphino)indol, min. 95% [cataCXium® PInCy] $C_{26}H_{32}NP$; FW: 389.51; white to yellow pwdr.   500mg 2g
air sensitive

Note: Sold in collaboration with Degussa for research purposes only. Patent Application pending.
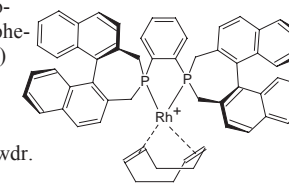
Technical Note:

1. See 15-3550 (page 41).

RHODIUM

96-6652   Degussa catASium® M Toolbox for Asymmetric Hydrogenation   1 kit
Contains 100mg unit of the following catASium® M items:

15-0108	45-0176	45-0754	45-0762	45-0770
45-0173	45-0750	45-0758	45-0766	45-0774

45-0795   (R,R)-(-)-1,2-Bis{(R)-4,5-dihydro-3H-binaphtho[1,2-c:2',1'-e]phosphepino}benzene(1,5-cyclooctadiene) rhodium (I) tetrafluoroborate (R)-BINAPHANE-Rh [Rh(C$_8$H$_{12}$)(C$_{50}$H$_{36}$P$_2$)]$^+$BF$_4^-$; FW: 1002.71; yellow to orange pwdr.   100mg 500mg
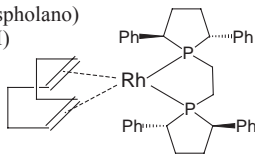*air sensitive*

Note: Sold in collaboration with Chiral Quest for research purposes only. Patent 6,525,210.
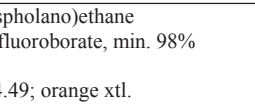
Technical Note:

1. See 15-0103 (Catalog 20 page 397).

RHODIUM (cont.)

45-0201   (-)-1,2-Bis((2R,5R)-2,5-diphenylphospholano) ethane(1,5-cyclooctadiene)rhodium (I) tetrafluoroborate, min. 98%   100mg 500mg 2g
(R,R)-Ph-BPE-Rh *[528565-84-6]*
$[Rh(C_8H_{12})(C_{34}H_{36}P_2)]^+BF_4^-$;
FW: 804.49; orange xtl.
air sensitive
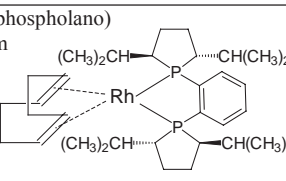
Note: Manufactured under US Patent 5,021,131 and US Patent 5,171,892.
Technical Note:
1. See 15-0473 (page 37).

45-0202   (+)-1,2-Bis((2S,5S)-2,5-diphenylphospholano)ethane (1,5-cyclooctadiene)rhodium (I) tetrafluoroborate, min. 98%   100mg 500mg 2g
(S,S)-Ph-BPE-Rh
$[Rh(C_8H_{12})(C_{34}H_{36}P_2)]^+BF_4^-$; FW: 804.49; orange xtl.
air sensitive
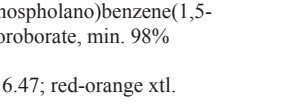
Note: Manufactured under US Patent 5,021,131 and US Patent 5,171,892.
Technical Note:
1. See 15-0473 (page 37).

45-0210   (+)-1,2-Bis((2R,5R)-2,5-di-i-propylphospholano) benzene(1,5-cyclooctadiene)rhodium (I) tetrafluoroborate, min. 98%   100mg 500mg 2g
(R,R)-i-Pr-DUPHOS-Rh
[569650-64-2]
$[Rh(C_8H_{12})(C_{26}H_{44}P_2)]^+BF_4^-$;
FW: 716.47; red-orange xtl.
air sensitive
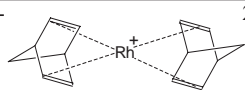
Note: Manufactured under US Patent 5,021,131 and US Patent 5,171,892.
Technical Note:
1. See 15-0096 (Catalog 20 page 398).

45-0211   (-)-1,2-Bis((2S,5S)-2,5-di-i-propylphospholano)benzene(1,5-cyclooctadiene) rhodium (I) tetrafluoroborate, min. 98%   100mg 500mg 2g
(S,S)-i-Pr-DUPHOS-Rh
$[Rh(C_8H_{12})(C_{26}H_{44}P_2)]^+BF_4^-$; FW: 716.47; red-orange xtl.
air sensitive

Note: Manufactured under US Patent 5,021,131 and US Patent 5,171,892.
Technical Note:
1. See 15-0096 (Catalog 20 page 398).

45-0230   Bis(norbornadiene)rhodium (I) tetrafluoro-borate, min. 96% *[36620-11-8]*   250mg 1g
$Rh(C_7H_8)_2^+BF_4^-$; FW: 373.99; red solid
air sensitive, (store cold)

Technical Note:
1. Precursor for asymmetric hydrogenation reactions.
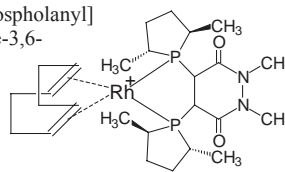
Reference:
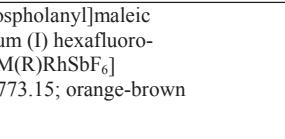1. *Angew. Chem. Int. Ed.*, **2002**, *41(24)*, 4708.

RHODIUM (cont.)

45-0750   (-)-4,5-Bis[(2R,5R)-2,5-dimethylphospholanyl] (1,2-dimethyl-1,2-dihydropyridazine-3,6-dione)(1,5-cyclooctadiene)rhodium (I) tetrafluoroborate, min. 95%   100mg 500mg
[catASium® MNN(R)Rh]
$Rh(C_8H_{12})(C_{18}H_{30}N_2O_2P_2)^+BF_4^-$;
FW: 666.28; orange-brown pwdr.
air sensitive

Note: Degussa catASium® M Toolbox Kit component. Sold in collaboration with Degussa for research purposes only. Patent WO 03084971.
Technical Note:
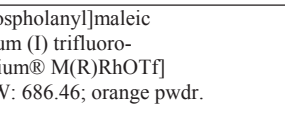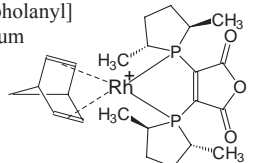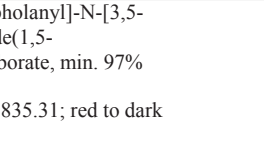1. See 45-0173 (Catalog 20 page 451).

45-0754   (-)-2,3-Bis[(2R,5R)-2,5-dimethylphospholanyl]maleic anhydride(1,5-cyclooctadiene)rhodium (I) hexafluoro-antimonate, min. 97% [catASium® M(R)RhSbF₆]   100mg 500mg
$Rh(C_8H_{12})(C_{16}H_{24}O_3P_2)^+SbF_6^-$; FW: 773.15; orange-brown pwdr.
air sensitive

Note: Degussa catASium® M Toolbox Kit component. Sold in collaboration with Degussa for research purposes only. Patent WO 03084971.
Technical Note:
1. See 45-0173 (Catalog 20 page 451).

45-0758   (-)-2,3-Bis[(2R,5R)-2,5-dimethylphospholanyl]maleic anhydride(1,5-cyclooctadiene)rhodium (I) trifluoro-methanesulfonate, min. 97% [catASium® M(R)RhOTf]   100mg 500mg
$Rh(C_8H_{12})(C_{16}H_{24}O_3P_2)^+CF_3SO_3^-$; FW: 686.46; orange pwdr.
air sensitive

Note: Degussa catASium® M Toolbox Kit component. Sold in collaboration with Degussa for research purposes only. Patent WO 03084971.
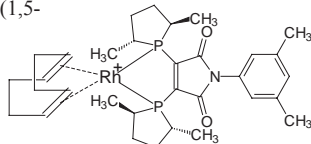Technical Note:
1. See 45-0173 (Catalog 20 page 451).

45-0762   (-)-2,3-Bis[(2R,5R)-2,5-dimethylphospholanyl] maleic anhydride(norbornadiene)rhodium (I) tetrafluoroborate, min. 97%   100mg 500mg
[catASium® M(R)RhNor]
$Rh(C_7H_8)(C_{16}H_{24}O_3P_2)^+BF_4^-$;
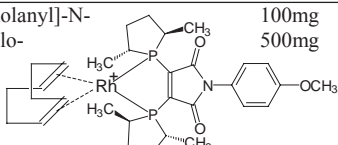FW: 608.16; orange pwdr.
air sensitive

Note: Degussa catASium® M Toolbox Kit component. Sold in collaboration with Degussa for research purposes only. Patent WO 03084971.
Technical Note:
1. See 45-0173 (Catalog 20 page 451).

45-0766   (-)-2,3-Bis[(2R,5R)-2,5-dimethylphospholanyl]-N-[3,5-bis(trifluoromethyl)phenyl]maleic imide(1,5-cyclooctadiene)rhodium (I) tetrafluoroborate, min. 97%   100mg 500mg
[catASium® MNMesF(R)Rh]
$Rh(C_8H_{12})(C_{24}H_{27}F_6NO_2P_2)^+BF_4^-$; FW: 835.31; red to dark red solid
*air sensitive*

Note: Degussa catASium® M Toolbox Kit component. Sold in collaboration with Degussa for research purposes only. Patent WO 03084971.
Technical Note:
1. See 45-0173 (Catalog 20 page 451).

RHODIUM (cont.)

45-0770   (-)-2,3-Bis[(2R,5R)-2,5-dimethylphospholanyl]-N-[3,5-dimethylphenyl]maleic imide(1,5-cyclooctadiene)rhodium (I) tetra-fluoroborate, min. 97% [catASium® MNMes(R)Rh] Rh(C$_8$H$_{12}$)(C$_{24}$H$_{33}$NO$_2$P$_2$)$^+$BF$_4^-$; FW: 727.36; red-brown solid   *air sensitive*   100mg / 500mg

Note: Degussa catASium® M Toolbox Kit component. Sold in collaboration with Degussa for research purposes only. Patent WO 03084971.
Technical Note:
   1. See 45-0173 (Catalog 20 page 451).

45-0774   (-)-2,3-Bis[(2R,5R)-2,5-dimethylphospholanyl]-N-[4-methoxyphenyl]maleic imide(1,5-cyclo-octadiene)rhodium (I) tetrafluoroborate, min. 97% [catASium® MNAn(R)Rh] Rh(C$_8$H$_{12}$)(C$_{23}$H$_{31}$NO$_3$P$_2$)$^+$BF$_4^-$; FW: 729.34; orange pwdr.   *air sensitive*   100mg / 500mg

Note: Degussa catASium® M Toolbox Kit component. Sold in collaboration with Degussa for research purposes only. Patent WO 03084971.
Technical Note:
   1. See 45-0173 (Catalog 20 page 451).

45-0653   (1S,1'S,2R,2'R)-(+)-1,1'-Di-t-butyl-[2,2']-diphospholane(1,5-cyclooocta-diene)rhodium (I) tetrafluoroborate, min. 98% (S,S,R,R)-TANGPHOS-Rh [Rh(C$_8$H$_{12}$)(C$_{16}$H$_{32}$P$_2$)]$^+$BF$_4^-$; FW: 608.29; orange xtl.   *air sensitive*   100mg / 500mg
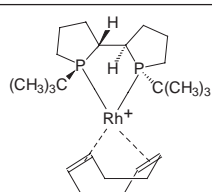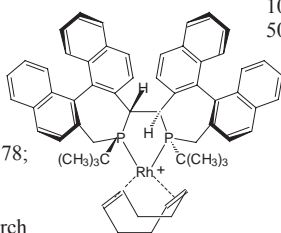
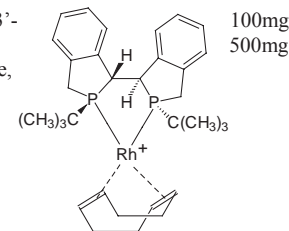Note: Sold in collaboration with Chiral Quest for research purposes only. Patent pending. PCT/US02/35788.
Technical Note:
   1. See 15-1015 (Catalog 20 page 419).

45-0657   (3S,3'S,4S,4'S,11bS,11'bS)-(+)-4,4'-Di-t-butyl-4,4',5,5'-tetrahydro-3,3'-bi-3H-dinaphtho[2,1-c:1',2'-e]phosphepin(1,5-cyclooctadiene)rhodium (I) tetrafluoroborate (S)-BINAPINE-Rh [Rh(C$_8$H$_{12}$)(C$_{52}$H$_{48}$P$_2$)]$^+$BF$_4^-$; FW: 1032.78; orange to brown pwdr.   *air sensitive*   100mg / 500mg

Note: Sold in collaboration with Chiral Quest for research purposes only. Patent pending, PCT/US02/35788.
Technical Note:
   1. See 15-1053 (Catalog 20 page 423).

RHODIUM (cont.)

45-0663   (1R,1'R,2S,2'S)-(+)-2,2'-Di-t-butyl-2,3,2',3'-tetrahydro-1,1'-bi-1H-isophosphindole(1,5-cyclooctadiene)rhodium (I) tetrafluoroborate, min. 98% (R,R,S,S)-DUANPHOS-Rh [Rh(C$_8$H$_{12}$)(C$_{24}$H$_{32}$P$_2$)]$^+$BF$_4^-$; FW: 680.35; orange xtl.   *air sensitive*   100mg / 500mg

Note: Sold in collaboration with Chiral Quest for research purposes only. Patent pending, PCT/US02/35788.
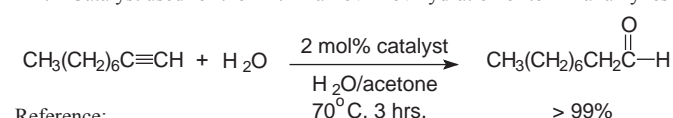Technical Note:
   1. See 15-1060 (page 38).

RUTHENIUM

44-0015   Acetonitrilebis[2-diphenylphosphino-6-t-butylpyridine]cyclopentadienyl-ruthenium (II) hexafluorophosphate, min. 98% *[776230-17-2]* Ru(C$_5$H$_5$)(CH$_3$CN)[C$_{21}$H$_{22}$NP]$_2^+$PF$_6^-$; FW: 990.94; yellow microxtl.   *air sensitive*   250mg / 1g
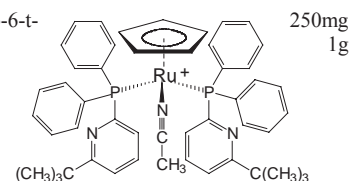
Technical Note:
   1. Catalyst used for the Anti-Markovnikov hydration of terminal alkynes to aldehydes.

$$CH_3(CH_2)_6C\equiv CH \ + \ H_2O \xrightarrow[\substack{H_2O/acetone \\ 70^\circ C, \ 3 \ hrs.}]{2 \ mol\% \ catalyst} CH_3(CH_2)_6CH_2C(=O)-H \quad > 99\%$$
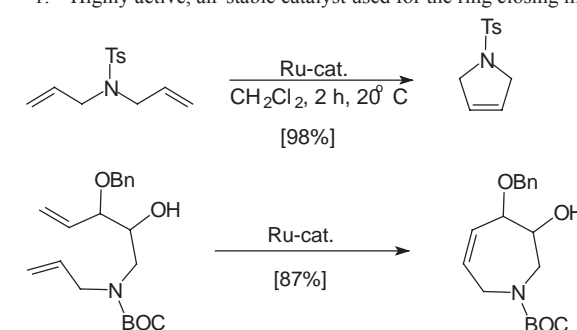
Reference:
   1. *J. Am. Chem. Soc.*, **2004**, *126*, 12232.

44-0063   Bis(tricyclohexylphosphine)-3-phenyl-1H-inden-1-ylideneruthenium dichloride Neolyst™ M1 *[250220-36-1]* RuCl$_2$(C$_{15}$H$_{10}$)[P(C$_6$H$_{11}$)$_3$]$_2$; FW: 923.07; brown pwdr.   1g / 5g
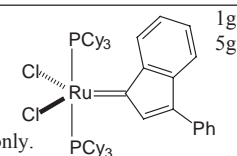
Note: Sold in collaboration with Umicore for research purposes only.
Technical Note:
   1. Highly active, air-stable catalyst used for the ring closing metathesis of dienes.
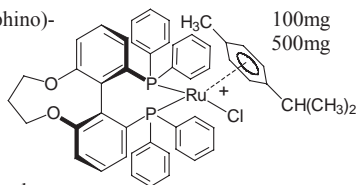
[98%]

[87%]

References:
   1. *Chem Eur. J.*, **2001**, *7*, 4811.
   2. *Angew. Chem. Int. Ed.*, **2000**, *112*, 3012. (review article)

RUTHENIUM

44-0109 Chloro{(R)-(-)-1,13-bis(diphenylphosphino)-7,8-dihydro-6H-dibenzo[f,h][1,5]dioxonin}(p-cymene)ruthenium (II) chloride (R)-C$_3$-TUNEPHOS-Ru [RuCl(C$_{39}$H$_{32}$O$_2$P$_2$)(C$_{10}$H$_{14}$)]$^+$Cl$^-$; FW: 900.81; orange to brown pwdr.
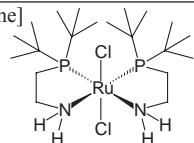*air sensitive*

100mg
500mg

Note: Sold in collaboration with Chiral Quest for research purposes only. Patent US 6,521,769.

Technical Note:
1. See 15-0175 (Catalog 20 page 408).

44-0260 Dichlorobis[2-(di-t-butylphosphino)ethylamine]ruthenium (II), min. 97% RuCl$_2$(C$_{10}$H$_{24}$NP)$_2$; FW: 550.53; orange pwdr.

250mg
1g

Note: Sold under license from Kanata for research purposes only. Patent WO0222526, EP1366004, US2004063966.
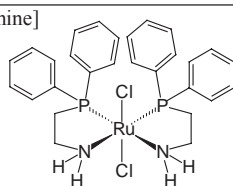
Technical Note:
1. Exceptionally active catalyst for the hydrogenation of ketones and imines under mild conditions. Selective hydrogenation of C=O bonds over C=C bonds.

neat
KO-t-Bu, rt
3 atms H$_2$
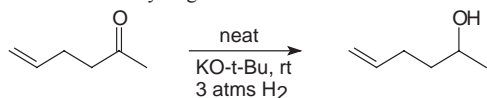
Reference:
1. *Adv. Synth. Catal.*, **2005**, *347*, 571.

44-0263 Dichlorobis[2-(diphenylphosphino)ethylamine]ruthenium (II), min. 95% RuCl$_2$(C$_{14}$H$_{32}$NP)$_2$; FW: 630.49; yellow pwdr.
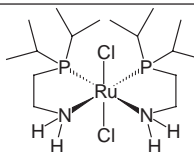
250mg
1g

Note: Sold under license from Kanata for research purposes only. Patents WO0222526, EP1366004, US2004063966.

Technical Note:
1. See 44-0260 (page 46).

44-0265 Dichlorobis[2-(di-i-propylphosphino)ethylamine]ruthenium (II), min. 97% RuCl$_2$(C$_8$H$_{20}$NP)$_2$; FW: 494.43; orange pwdr.

250mg
1g

Note: Sold under license from Kanata for research purposes only. Patents WO0222526, EP1366004, US2004063966.

Technical Note:
1. See 44-0260 (page 46).

44-0381 Dichloro[(S)-(+)-4,12-bis(di(3,5-xylyl)phosphino)-[2.2]-paracyclophane][(1R,2R)-(+)-1,2-diphenylethylene-diamine]ruthenium (II), min. 95% RuCl$_2$[C$_{48}$H$_{50}$P$_2$][C$_{14}$H$_{16}$N$_2$]; FW: 1073.12; cream colored pwdr.
air sensitive

10mg
50mg
250mg

RUTHENIUM (cont.)

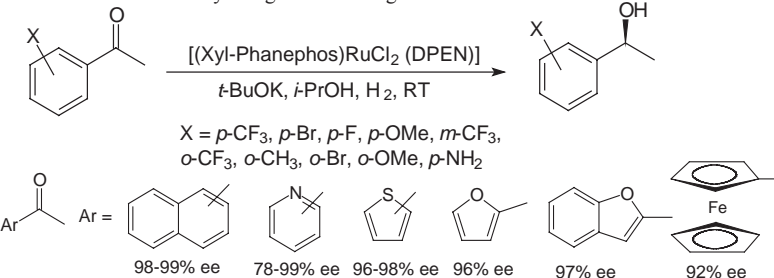**44-0381 (cont.)** Dichloro[(S)-(+)-4,12-bis(di(3,5-xylyl)phosphino)-[2.2]-paracyclophane][(1R,2R)-(+)-1,2-diphenylethylenediamine]ruthenium (II), min. 95%
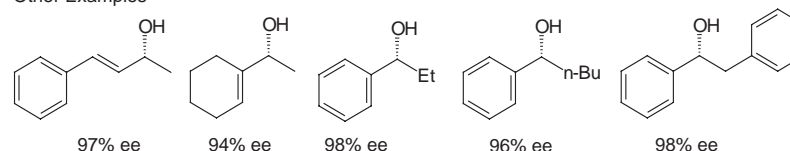
Note: Sold in collaboration with Chirotech for research purposes only. US Patent nos. 5874629 and 6486337.

Technical Notes:
1. The Noyori [(diphosphine) RuCl$_2$ (diamine)] catalysts containing the chiral ligand Xylyl-Phanephos display exceptional activity and enantioselectivity in the asymmetric hydrogenation of a wide range of aromatic, heteroaromatic and α,β-unsaturated ketones.
2. Reactions are performed under mild conditions at room temperature and typically at low H$_2$ pressures of 2-10 bar. High substrate concentrations of up to 40% w/v are tolerated.
3. Molar substrate/catalyst ratios of up to 100,000/1 are achieved with excellent reactivity and enantioselectivity using commercial grade substrates and solvents.

[(Xyl-Phanephos)RuCl$_2$ (DPEN)]
t-BuOK, i-PrOH, H$_2$, RT

X = p-CF$_3$, p-Br, p-F, p-OMe, m-CF$_3$, o-CF$_3$, o-CH$_3$, o-Br, o-OMe, p-NH$_2$

Ar =

98-99% ee   78-99% ee   96-98% ee   96% ee   97% ee   92% ee

Other Examples

97% ee   94% ee   98% ee   96% ee   98% ee

References:
1. *Org. Lett.*, **2000**, *2*, 4173.
2. Burk, M.J.; Hems, W.; Zanotti-Gerosa, A. PCT WO/0174829 A1, **2001**.
3. *Org. Proc. Res. Dev.*, **2003**, 7, 89.

44-7890 Tris(acetonitrile)pentamethylcyclopentadienylruthenium (II) trifluoromethanesulfonate, min. 98% *[113860-02-9]* [Ru(C$_{10}$H$_{15}$)(CH$_3$CN)$_3$]$^+$CF$_3$SO$_3^-$; FW: 508.52; orange pwdr.
air sensitive, (store cold)

250mg
1g

Technical Note:
1. See 44-7870 (Catalog 20 page 468).

TUNGSTEN

74-1800 Tris(t-butoxy)(2,2-dimethylpropylidyne) tungsten (VI), 98% Schrock Alkyne Metathesis Catalyst *[78234-36-3]* (C$_4$H$_9$O)$_3$W≡CC(CH$_3$)$_3$; FW: 472.31; off-white to tan pwdr.
air sensitive, moisture sensitive, (store cold)

100mg
500mg

(CH$_3$)$_3$CO
(CH$_3$)$_3$CO—W≡C—C(CH$_3$)$_3$
(CH$_3$)$_3$CO
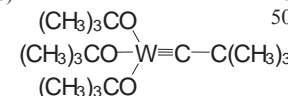
TUNGSTEN (cont.)

74-1800 (cont.)	Tris(t-butoxy)(2,2-dimethylpropylidyne)tungsten (VI), 98% Schrock Alkyne Metathesis Catalyst [78234-36-3]

Technical Note:

1. A well-defined, tungsten-based alkyne metathesis, catalyst first prepared by Professor Richard Schrock. The catalyst has been used to prepare a variety of products through alkyne metathesis, including natural products that contain large rings.

78%

Ref. (3)

1. Ac$_2$O, H$^+$
2. deprotection

Citreofuran
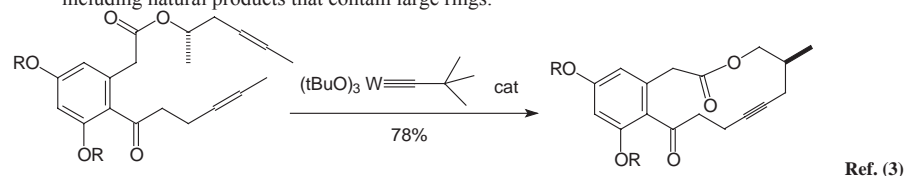
References:

1. *Acc. Chem. Res.*, **1986**, *19*, 342. (review article)
2. *Angew. Chem. Int. Ed.*, **2000**, *39*, 3012. (review article)
3. *J. Org. Chem.*, **2003**, *68*, 1521.

ZIRCONIUM

40-1056	(+)-Bis[1-{(1'R,2'R,5'R)-2'-i-propyl-5'-methylcyclohexyl}indenyl]zirconium (IV) dichloride [148347-90-4]	100mg 500mg

(C$_{19}$H$_{25}$)$_2$ZrCl$_2$; FW: 668.93; orange pwdr.; [α]$_D$ +71°
(c 0.28, toluene)
moisture sensitive

Technical Note:

1. See 40-1057 (page 48).

40-1057	(-)-Bis[1-{(1'S,2'S,5'R)-2'-i-propyl-5'-methyl-cyclohexyl}indenyl]zirconium (IV) dichloride [148347-88-0]	100mg 500mg

(C$_{19}$H$_{25}$)$_2$ZrCl$_2$; FW: 668.93; orange pwdr.;
[α]$_D$ −77° (c 0.23, toluene)
moisture sensitive
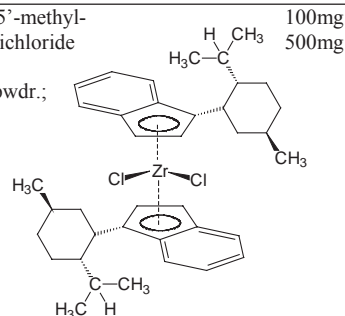
Technical Notes:

1. Catalyst used for the enantioselective carboalumination of unactivated alkenes.
2. Catalyst used for the enantioselective synthesis of methyl-substituted alkanols and their derivatives.

ZIRCONIUM (cont.)

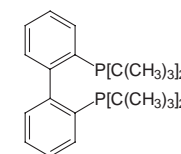| 40-1057 (cont.)	(-)-Bis[1-{(1'S,2'S,5'R)-2'-i-propyl-5'-methylcyclohexyl}indenyl]zirconium (IV) dichloride [148347-88-0]
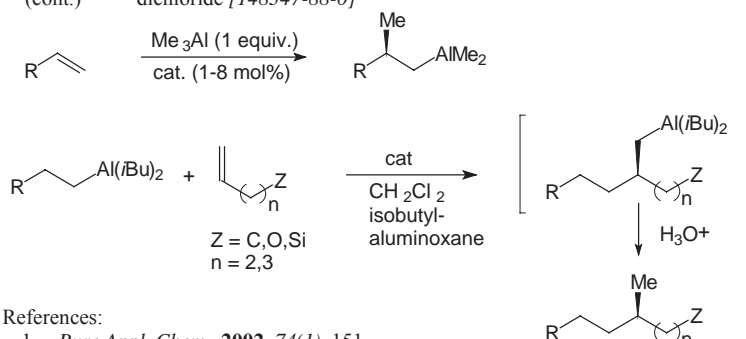
References:

1. *Pure Appl. Chem.*, **2002**, *74(1)*, 151.
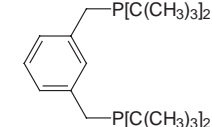2. *Angew. Chem. Int. Ed.*, **2002**, *41*, 2141.

PHOSPHORUS COMPOUNDS

15-0071	2,2'-Bis(di-t-butylphosphino)-1,1'-biphenyl, min. 97% C$_{28}$H$_{44}$P$_2$; FW: 442.60; white to pale yellow pwdr.		250mg 1g
15-0065	1,3-Bis(di-t-butylphosphinomethyl) benzene, 99% [149968-36-5] C$_6$H$_4$[CH$_2$P(C$_4$H$_9$)$_2$]$_2$; FW: 394.56; white pwdr. *air sensitive*		250mg 1g
15-9560	2,2'-Bis(dicyclohexylphosphino)-1,1'-biphenyl, min. 97% [255897-36-0] C$_{36}$H$_{52}$P$_2$; FW: 546.75; white to pale yellow pwdr.		250mg 1g
15-9595	1,3-Bis(dicyclopentylphosphinomethyl) benzene, 99% [255874-48-7] C$_6$H$_4$[CH$_2$P(C$_5$H$_9$)$_2$]$_2$; FW: 442.60; white, waxy solid *air sensitive*		250mg 1g
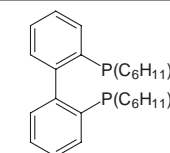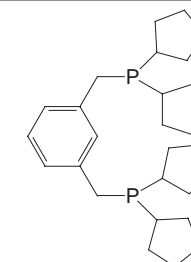
PHOSPHORUS COMPOUNDS (cont.)

15-0481	(R,R)-(-)-1,2-Bis[(2-methoxyphenyl)(phenyl) phosphino]ethane, 98% (-)-DIPAMP [55739-58-7] ($C_6H_4OCH_3$)(C_6H_5)PCH$_2$CH$_2$P($C_6H_4OCH_3$) (C_6H_5); FW: 458.47; white xtl.; m.p. 102-103°; [α]$_D$ –87° (c 1.0, CHCl$_3$)	250mg 1g

Technical Note:
1. Rhodium DIPAMP catalysts have shown high activity and enantioselectivity in the asymmetric hydrogenation of enamides, enol acetates and olefins.

References:
1. *ACS Symposium Series*, **1993**, *517* (Selectivity in Catalysis), 58-74 (review).
2. *Acc. Chem. Res.*, **1983**, *16*, 106 (review).

15-0482	(S,S)-(+)-1,2-Bis[(2-methoxyphenyl)(phenyl)phosphino] ethane, 98% (+)-DIPAMP [97858-62-3] ($C_6H_4OCH_3$)(C_6H_5)PCH$_2$CH$_2$P($C_6H_4OCH_3$)(C_6H_5); FW: 458.47; white xtl.; m.p. 102-103°; [α]$_D$ +87° (c 1.0, CHCl$_3$)	250mg 1g

Technical Note:
1. See 15-0481 (page 50).

15-1827	Diphenyl(m-sulfonatophenyl)phosphine dihydrate sodium salt, min. 97% [63995-75-5] (C_6H_5)$_2$P($C_6H_4SO_3Na$) 2H$_2$O; FW: 364.33 (400.36); white pwdr.	1g 5g

Technical Note:
1. A water-soluble phosphine ligand used in the formation of water-soluble catalysts.

15-1825	Diphenyl(p-sulfonatophenyl)phosphine monohydrate dimethylsulfoxide adduct, potassium salt (C_6H_5)$_2$P($C_6H_4SO_3K$) H$_2$O CH$_3$SOCH$_3$; FW: 380.44 (476.59); white pwdr.	1g 5g

Note: A water soluble phosphine.

15-1795	Di-i-propylphosphine, 98% [20491-53-6] (C_3H_7)$_2$PH; FW: 118.16; colorless liq. *air sensitive, pyrophoric*	1g 5g
15-1819	Di-p-tolylphosphine, 99% (10 wt% in hexane) [1017-60-3] (CH$_3$C$_6$H$_4$)$_2$PH; FW: 214.25; colorless liq. *air sensitive*	20g 100g
15-5813	Tri-t-butylphosphine, min. 98% [13716-12-6] (t-C$_4$H$_9$)$_3$P; FW: 202.32; colorless liq. to white solid; m.p. 30°; b.p. 102-103°/13mm; f.p. 1°F ; d. 0.812 *pyrophoric*	1g 5g

METALS SCAVENGING AGENTS

96-6700	Engelhard Metals Scavenging Agent Kit Contains 10g unit of the four items listed below.	1 kit
13-6300	Metals scavenging agent, Phosphotungstic acid modified alumina (Engelhard MSA-FC Al-1) d50=159µm; white pwdr.; d. 1.00 g/ml	10g 50g
06-0805	Metals scavenging agent, Phosphotungstic acid modified activated carbon (Engelhard MSA-FC C-1) d50=27µm; black pwdr.; d. 0.60 g/ml	10g 50g
14-4351	Metals scavenging agent, Ethylenediamine modified silica (Engelhard MSA-FC Si-1) d50=83µm; white to slightly yellow pwdr.; d. 0.88 g/ml	10g 50g

METALS SCAVENGING AGENTS (cont.)

14-4353	Metals scavenging agent, Mercaptopropyl modified silica (Engelhard MSA-FC Si-3) d50=83µm; white to slightly yellow pwdr.; d. 0.88 g/ml	10g 50g

Sold for research purposes only in collaboration with Engelhard. Commercial quantities available from Engelhard.

Metal scavenging agents are air and water stable.

OTHER NEW PRODUCTS

ALUMINUM

13-1600	Dimethylaluminum i-propoxide, 98% (99.99+%-Al) [6063-89-4] (CH$_3$)$_2$Al(OC$_3$H$_7$); FW: 116.14; colorless liq. *air sensitive, moisture sensitive*	1g 5g

Technical Note:
1. Useful starting material for the atomic layer deposition of Al$_2$O$_3$ films.

CARBON

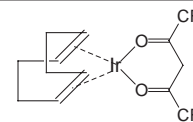|		
06-0150	t-Butylmethylacetylene, 99% [999-78-0] C$_4$H$_9$C≡C(CH$_3$); FW: 96.17; colorless liq.; b.p. 83°; f.p. 14°F	1g 5g
06-0526	Fullerene-C$_{76}$, min. 98% [135113-15-4] C$_{76}$; FW: 912.84; black pwdr.	5mg

IRIDIUM

77-0250	Chlorobis(cyclooctene)iridium (I) dimer, 97% [12246-51-4] [IrCl(C$_8$H$_{14}$)$_2$]$_2$; FW: 896.13; yellow xtl. *moisture sensitive*	250mg 1g

Technical Note:
1. Useful starting material for preparing iridium catalysts.

77-0930	1,5-Cyclooctadiene(hexafluoro-acetylacetonato)iridium (I), 98% [34801-95-1] Ir(C$_8$H$_{12}$)(C$_5$HF$_6$O$_2$); FW: 507.45; red-purple xtl.	100mg 500mg
77-0950	1,5-Cyclooctadiene(h5-indenyl)iridium (I), 99% [102525-11-1] C$_{17}$H$_{19}$Ir; FW: 415.55; yellow xtl.	250mg 1g

IRON

26-2801	Iron pentacarbonyl, 99.5% (Sure/Seal™ bottle) [13463-40-6] Fe(CO)$_5$; FW: 195.90; orange liq.; m.p. –20°; b.p. 103°; f.p. 5°F; d. 1.490 *air sensitive, (store cold)*	250g 1kg

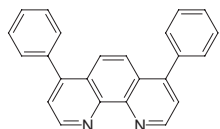### NITROGEN

07-0595	1,3-Bis(2,6-di-i-propylphenyl)imidazol-2-ylidene, min. 98% [244187-81-3] C$_{27}$H$_{36}$N$_2$; FW: 388.59; white to off-white pwdr.	500mg 2g
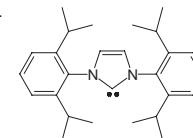
NITROGEN

07-0472   4,7-Diphenyl-1,10-phenanthroline,   250mg
min. 97% (Bathophenanthroline)   1g
[1662-01-7]
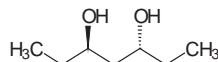$C_{24}H_{16}N_2$; FW: 332.40; off-white pwdr.;
m.p. 218°

Technical Note:
1. Bidentate ligand and reagent for determination of iron.

OXYGEN

08-2014   (3R,5R)-(-)-3,5-Heptanediol, 99%   250mg
[77291-90-8]   1g
$C_7H_{16}O_2$; FW: 132.20;
colorless solid; $[\alpha]_D$ –40° (c 10, ethanol)

08-2015   (3S,5S)-(+)-3,5-Heptanediol, 99% *[129212-21-1]*   250mg
$C_7H_{16}O_2$; FW: 132.20; colorless solid; $[\alpha]_D$ +40°   1g
(c 10, ethanol)

08-2037   (3R,6R)-(-)-3,6-Octanediol, 99% *[129619-37-0]*   250mg
$C_2H_5C(OH)CH_2CH_2C(OH)C_2H_5$; FW: 146.23; colorless xtl.;   1g
$[\alpha]_D$ -15° (c 10, ethanol)

08-2038   (3S,6S)-(+)-3,6-Octanediol, 99% *[136705-66-3]*   250mg
$C_2H_5C(OH)CH_2CH_2C(OH)C_2H_5$; FW: 146.23; colorless xtl.;   1g
$[\alpha]_D$ +15° (c 10, ethanol)

PLATINUM

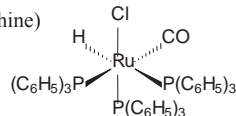78-1300   (Trimethyl)cyclopentadienylplatinum (IV), 99%   500mg
[1271-07-4]   2g
$(CH_3)_3(C_5H_5)Pt$; FW: 305.28; white to off-white pwdr.; m.p.
104-106°
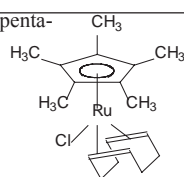*air sensitive*

RUTHENIUM

44-0085   Carbonylchlorohydridotris(triphenylphosphine)   1g
ruthenium (II), 99% *[16971-33-8]*   5g
$Ru(CO)ClH[P(C_6H_5)_3]_3$;
FW: 952.40; off-white to
tan pwdr.; m.p. 209-210°

44-0113   Chloro(1,5-cyclooctadiene)(pentamethylcyclopenta-   250mg
dienyl)ruthenium (II), 98% *[92390-26-6]*   1g
$RuCl(C_8H_{12})(C_{10}H_{15})$; FW: 379.93

RUTHENIUM

44-0116   Chloro(cyclopentadienyl)[bis(diphenylphosphino)   250mg
methane]ruthenium (II), min. 97% *[71397-33-6]*   1g
$RuCl(C_5H_5)[(C_6H_5)_2PCH_2P(C_6H_5)_2]$;
FW: 586.01; orange xtl.
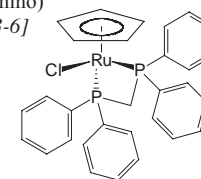
Technical Note:
1. Useful catalyst for the anti-Markovnikov hydration
of terminal alkynes.
Reference:
1. *Org. Lett.*, **2001**, *3*, 735.

SODIUM

11-0590   Sodium tetrakis[3,5-bis(trifluoromethyl)phenyl]borate,   250mg
min. 98% *[79060-88-1]*   1g
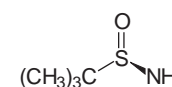$Na^+[B(C_6H_3(CF_3)_2)_4]^-$; FW: 886.20; tan pwdr.

Note: May contain <5 mole% water and <5 mole% residual ethers.

SULFUR

16-0380   (R)-(+)-t-Butylmethylsulfinamide, min. 97%   1g
[196929-78-9]   5g
$(C_4H_9)(CH_3)S(O)NH_2$; FW: 121.20; white pwdr.;
m.p. 103-107°; $[\alpha]_D$ +4° (c 1.2, $CHCl_3$)
(store cold)

Technical Note:
1. Useful reagent for synthesizing chiral amines.
References:
1. *Acc. Chem. Res.*, **2002**, *35*, 984.
2. *Chem. Soc. Rev.*, **1998**, *27*, 13.

16-0381   (S)-(-)-t-Butylmethylsulfinamide, min. 97% *[343338-28-3]*   1g
$(C_4H_9)(CH_3)S(O)NH_2$; FW: 121.20; white pwdr.; m.p. 97-101°;   5g
$[\alpha]_D$ –4.5° (c 1.0, $CHCl_3$)
(store cold)

Technical Note:
1. See 16-0380 (page 53).

TIN

50-4200   Tri-i-propyltin chloride, min. 98% *[14101-95-2]*   1g
$(C_3H_7)_3SnCl$; FW: 238.43; colorless liq.   5g

THE STREM CHEMIKER

STREM CHEMICALS, INC.

7 Mulliken Way
Newburyport, MA 01950-4098 U.S.A.
Tel.: (978) 462-3191   Fax: (978) 465-3104
(Toll-free numbers below US & Canada only)
Tel.: (800) 647-8736   Fax: (800) 517-8736

OUR LINE OF RESEARCH CHEMICALS

Electronic grade chemicals
Fullerenes
High purity inorganics and alkali metals
Ionic liquids
Ligands and chiral ligands
Metal acetates and carbonates
Metal alkoxides and beta-diketonates
Metal alkyls and alkylamides
Metal carbonyls and derivatives
Metal catalysts and chiral catalysts
Metal foils, wires, powders and elements
Metal halides, hydrides and deuterides
Metal oxides, nitrates and chalcogenides
Metallocenes
Nanomaterials
Organofluorines
Organometallics
Organophosphines and arsines
Porphines and phthalocyanines
Precious metal and rare earth chemicals
Volatile precursors for MOCVD and CVD
Bulk Manufacturing, Custom Synthesis
cGMP facilities

Searchable catalog at www.strem.com